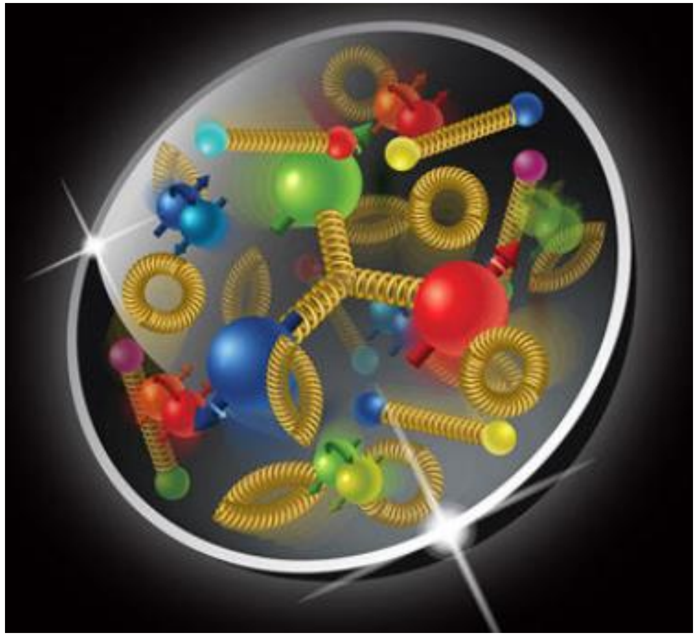

Lesson III: Hadronic scale, experimental point of view:

From high-energy lepton scattering to nucleon pressure

After the introduction of the different types of experiments to reveal the nucleon structure, the focus is on Exclusive Reactions related to GPDs:

- ✓ **Correlation between position and momentum of partons**
- ✓ **Angular momentum and nucleon pressure**

Nicole d'Hose (Irfu, CEA Université Paris-Saclay)

Since the proton is composed of quarks confined by gluons, an equivalent pressure which acts on the quarks can be defined. This allows calculation of their distribution as a function of distance from the momentum centre using **Deeply Virtual Compton Scattering**.

Deeply virtual Compton scattering (DVCS)

D. Mueller *et al*, Fortsch. Phys. 42 (1994)
X.D. Ji, PRL 78 (1997), PRD 55 (1997)
A. V. Radyushkin, PLB 385 (1996), PRD 56 (1997)

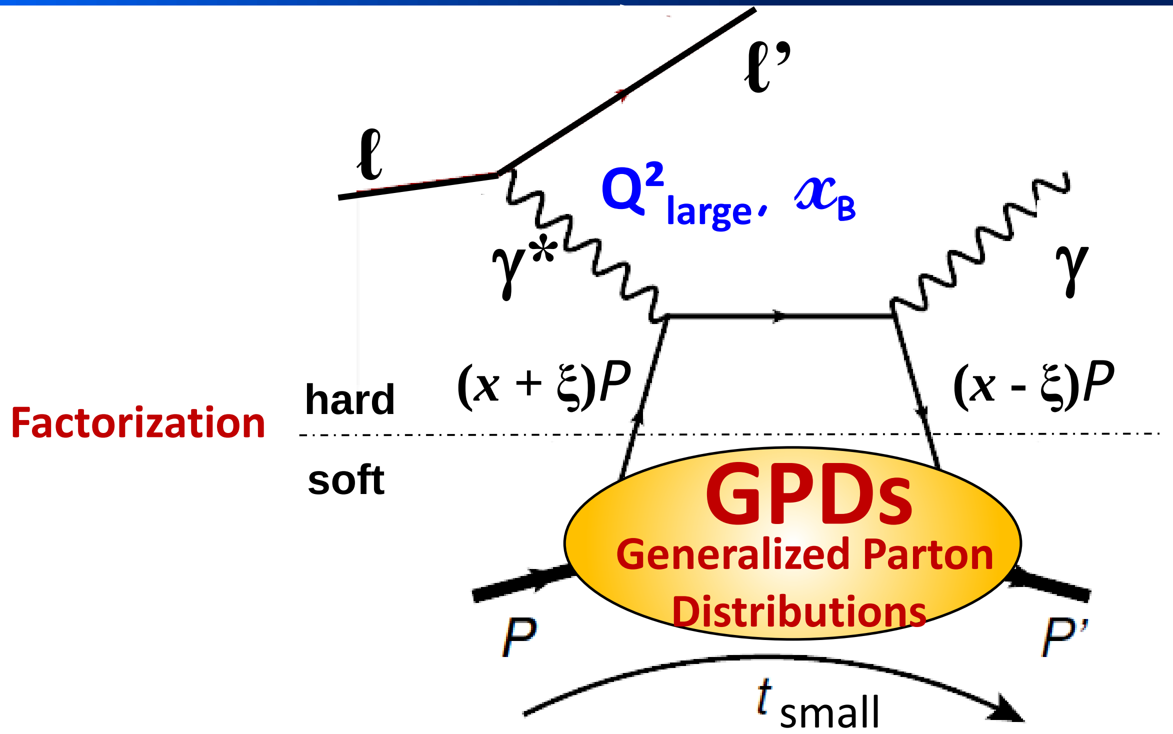

DVCS: $\ell p \rightarrow \ell' p' \gamma$
the golden channel
because it interferes with
the Bethe-Heitler process

also meson production
$\ell p \rightarrow \ell' p' \pi, \rho, \omega$ or ϕ or J/ψ...

The GPDs depend on the following variables:

x: average
ξ: transferred
} quark longitudinal momentum fraction

t: proton momentum transfer squared
related to $b_\perp$ via Fourier transform
Q^2: virtuality of the virtual photon

The variables measured in the experiment:

E_ℓ, Q^2, $x_B \sim 2\xi/(1+\xi)$,
t (or $\theta_{\gamma^*\gamma}$) and ϕ ($\ell\ell'$ plane/$\gamma\gamma^*$ plane)

Deeply virtual Compton scattering (DVCS)

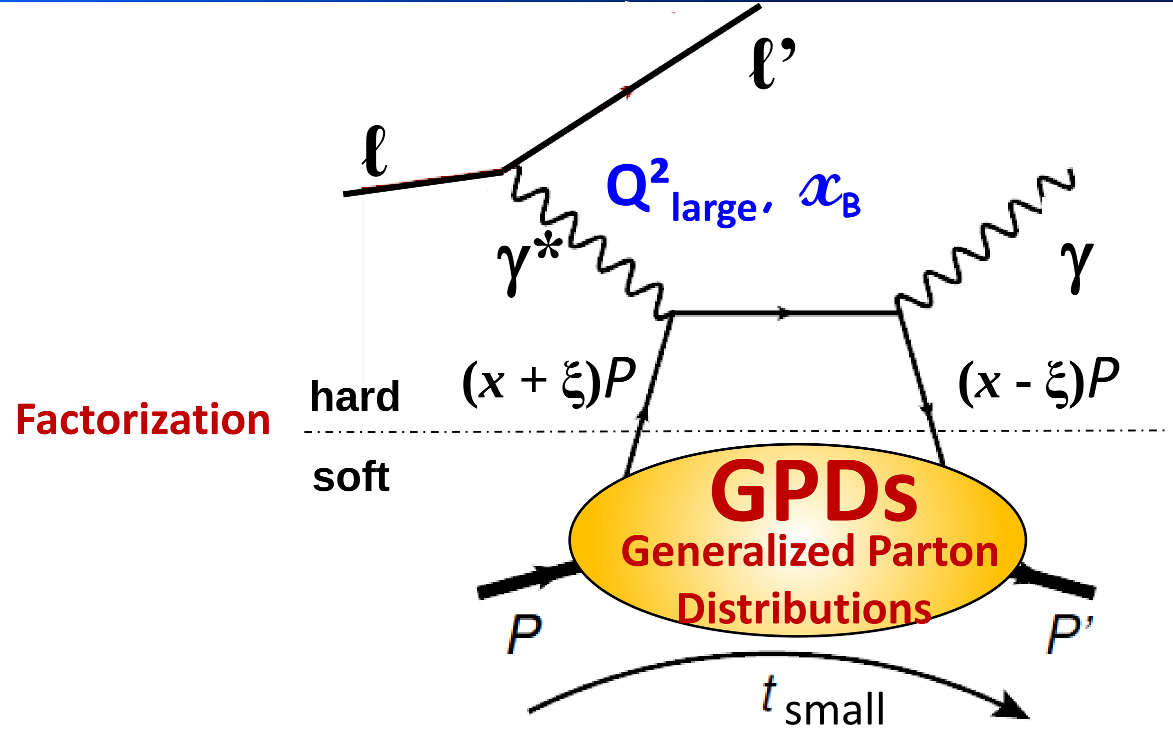

Goeke, Polyakov, Vanderhaeghen, PPNP47 (2001)

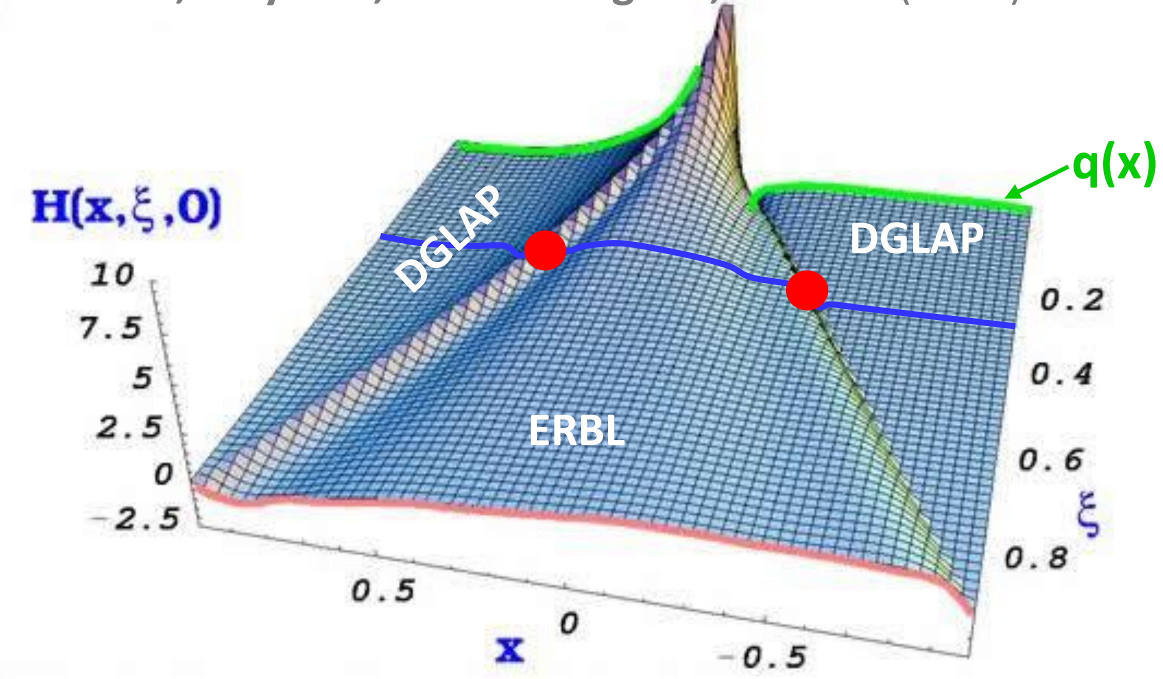

The amplitude DVCS at LT & LO in α_s (GPD **H**) :

Real part Imaginary part

$$\underset{t,\,\xi\ \text{fixed}}{\mathcal{H}} = \int_{-1}^{+1} dx\, \frac{H(x,\xi,t)}{x-\xi+i\varepsilon} = \mathcal{P}\int_{-1}^{+1} dx\, \frac{H(x,\xi,t)}{x-\xi} - i\,\pi\, H(x=\pm\xi,\xi,t)$$

In an experiment we measure

Compton Form Factor $\mathcal{H}$

$$\mathcal{R}e\mathcal{H}(\xi,t) = \pi^{-1}\int_0^1 dx\, \frac{2x\ Im\mathcal{H}(x,t)}{x^2-\xi^2} + \Delta(t)$$

Deeply virtual Compton scattering (DVCS)

M. Burkardt, PRD66(2002)

M. Polyakov, P. Schweitzer, Int.J.Mod.Phys. A33 (2018)

Mapping in the transverse plane

$q(x, b_\perp)$

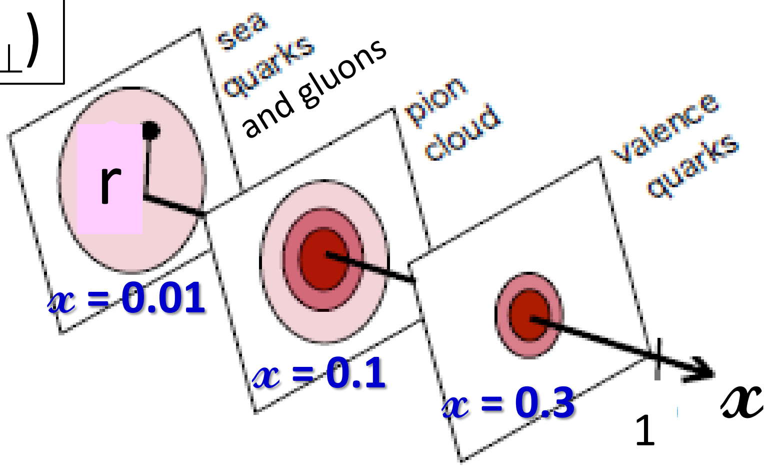

FT of H(x, ξ=0,t)

Pressure Distribution

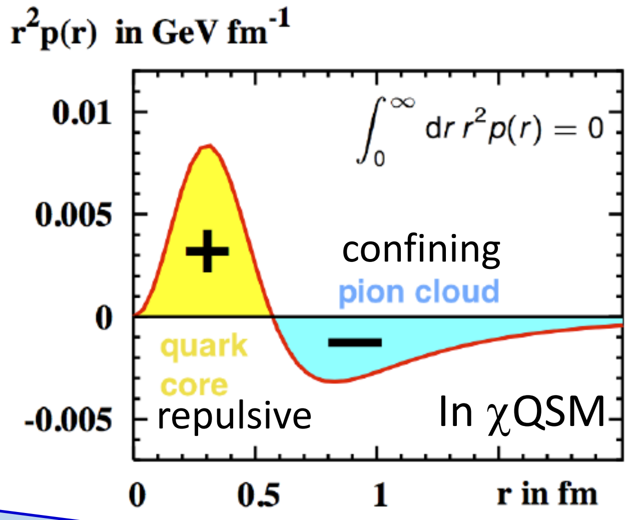

The amplitude DVCS at LT & LO in α_s (GPD **H**) :

Real part **Imaginary part**

$$\mathcal{H} = \int_{-1}^{+1} dx \, \frac{H(x,\xi,t)}{x-\xi+i\varepsilon} = \mathcal{P}\int_{-1}^{+1} dx \, \frac{H(x,\xi,t)}{x-\xi} - i\pi H(x=\pm\xi,\xi,t)$$

t, ξ fixed

In an experiment we measure

Compton Form Factor $\mathcal{H}$

$$Re\mathcal{H}(\xi,t) = \pi^{-1}\int_0^1 dx \, \frac{2x \, Im\mathcal{H}(x,t)}{x^2-\xi^2} + \Delta(t)$$

D-term

$d_1(t)$

GPDs and Energy-Momentum Tensor and Confinement

GPDs can provide an experimental answer by exploiting their equivalence to the gravitational form factors of the nucleon energy-momentum-tensor (fundamental nucleon properties)

$$\int_{-1}^{1} dx\, x\, H^a(x,\xi,t) = A^a(t) + \xi^2 d_1^a(t)$$

$$\int_{-1}^{1} dx\, x\, E^a(x,\xi,t) = 2J^a(t) - A^a(t) - \xi^2 d_1^a(t)$$

mass & energy distribution ($A^a(t)$)

Angular momentum distribution ($J^a(t)$)

Force & Pressure distribution ($d_1^a(t)$)

M. Polyakov et al. Phys.Rev. D75 (2007)
Int.J.Mod.Phys. A33 (2018)

$$2J^q = \lim_{t\to 0} \int x\,(H^q(x,\xi,t) + E^q(x,\xi,t))\,dx$$

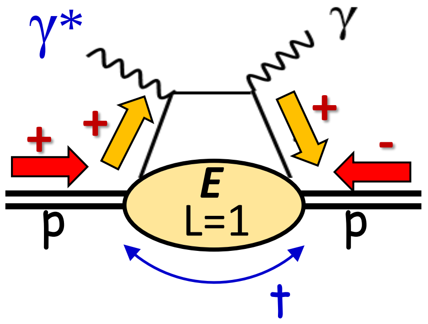

Relation to OAM

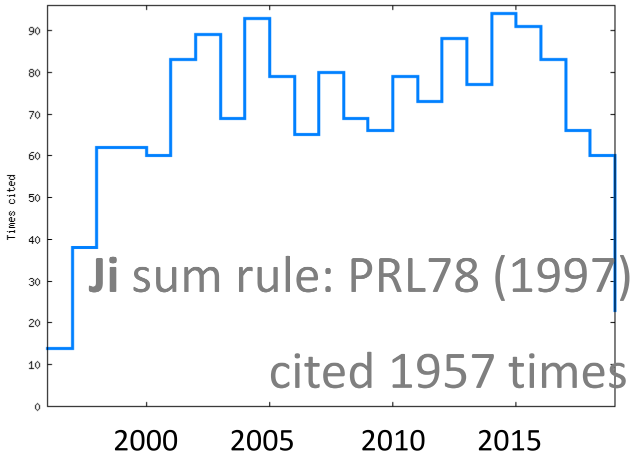

Pressure Distribution

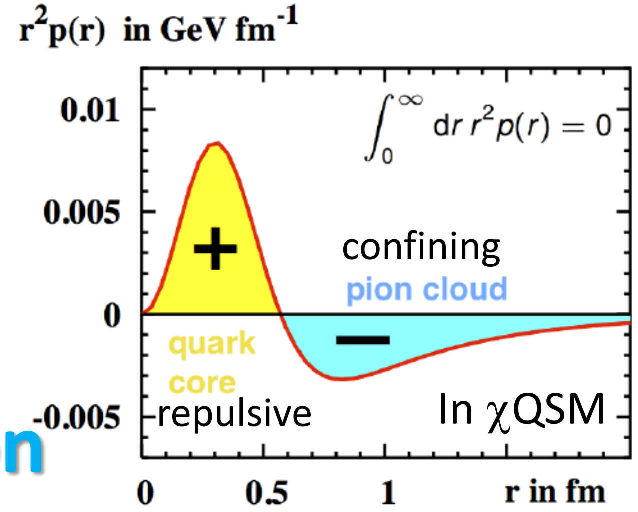

The pion field provides the confining pressure at the proton periphery (pions are the Goldstone bosons of the spontaneous chiral symmetry breaking)

Confinement and Pressure

Since the proton is composed of quarks confined by gluons, an equivalent pressure which acts on the quarks can be defined. This allows calculation of their distribution as a function of distance from the centre using **Deeply Virtual Compton Scattering.** It has been shown in a first publication in Nature that the pressure is maximum at the centre, about 10^{35} Pa, which is greater than the pressure inside a neutron star. It is **positive (repulsive)** to a distance of about 0.6 fm, **negative (attractive, confining)** at greater distances, and very weak beyond about 2 fm.

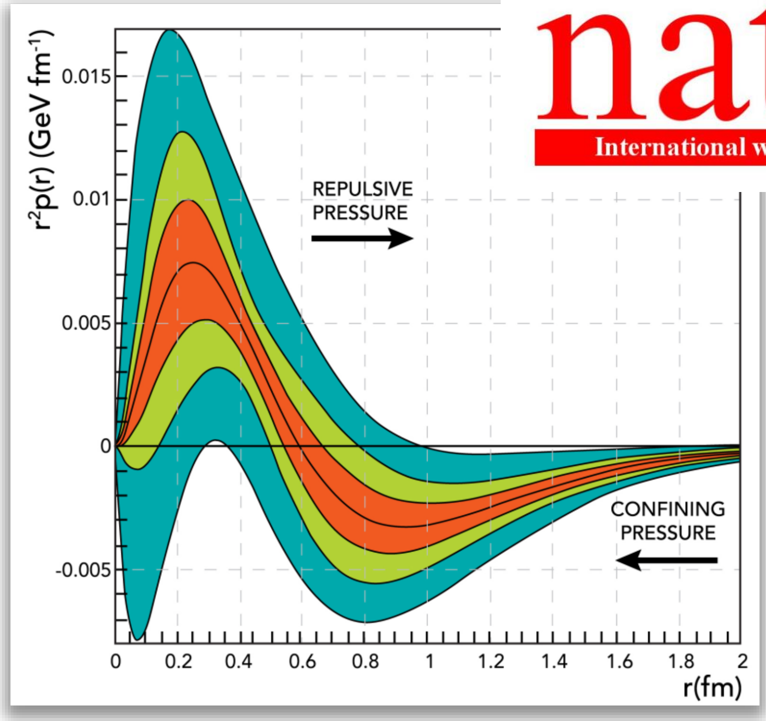

nature
International weekly journal of science

LETTER

https://doi.org/10.1038/s41586-018-0060-z

The pressure distribution inside the proton

V. D. Burkert[1]*, L. Elouadrhiri[1] & F. X. Girod[1]

16 May 2018

1eV = 1.6 10^{-19} Nm   1 Pa=N/m^2

Near the center at r=0.05fm $r^2p=10^{-3}$ GeV fm^{-1}

➔ $p=10^{-3} \cdot 1.6\ 10^{-19} \cdot 10^{9} \cdot (10^{15})^3 / (0.05)^2 = 0.640\ 10^{35}$ Pa

Repulsive pressure near center   **p(r=0) ~ 10^{35} Pa**

Atmospheric pressure: 10^5 Pa

Pressure in the center of neutron stars ~ 10^{35} Pa

Confinement and Pressure

Since the proton is composed of quarks confined by gluons, an equivalent pressure which acts on the quarks can be defined. This allows calculation of their distribution as a function of distance from the centre using **Deeply Virtual Compton Scattering.** It has been shown in a first publication in Nature that the pressure is maximum at the centre, about 10^{35} Pa, which is greater than the pressure inside a neutron star. It is positive (repulsive) to a radial distance of about 0.6 fm, negative (attractive) at greater distances, and very weak beyond about 2 fm.

This work was revisited after. The experimental method (**direct extraction of physical observable)** is not questioned but the evaluation of the incertainties is. With the present set of data the high pressure in the center is also compatible with 0.

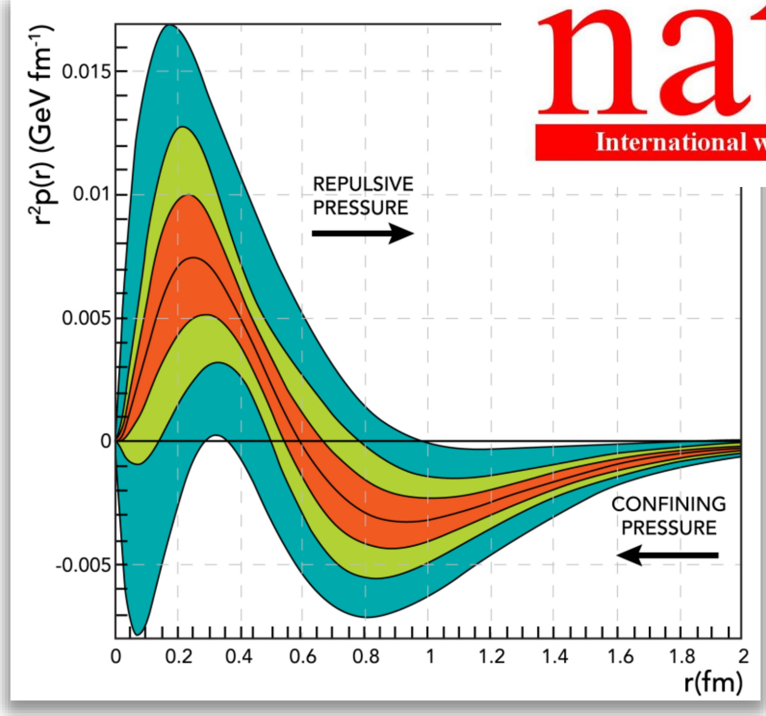

nature
International weekly journal of science

LETTER

https://doi.org/10.1038/s41586-018-0060-z

The pressure distribution inside the proton

V. D. Burkert[1]*, L. Elouadrhiri[1] & F. X. Girod[1]

16 May 2018

MATTERS ARISING

https://doi.org/10.1038/s41586-019-1211-6

Measurability of pressure inside the proton

Krešimir Kumerički[1]*

05 June 2019

Eur. Phys. J. C (2019) 79:614
https://doi.org/10.1140/epjc/s10052-019-7117-5

THE EUROPEAN PHYSICAL JOURNAL C

Unbiased determination of DVCS Compton form factors

H. Moutarde[1,a], P. Sznajder[2,b], J. Wagner[2,c]

20 July 2019

Confinement and Pressure

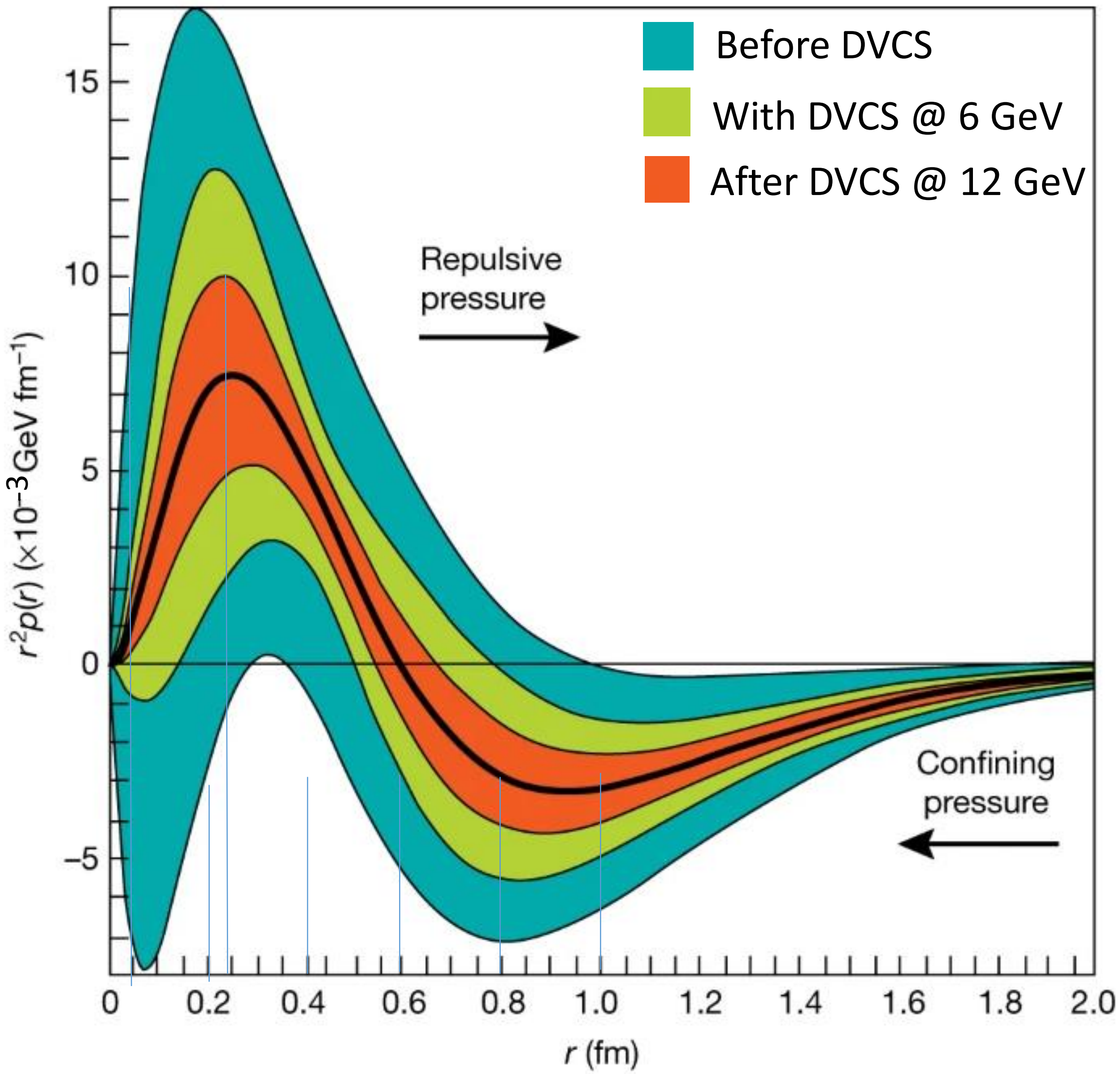

Radial pressure distribution in the proton.

The graph shows the pressure distribution r2 p(r) that results from the interactions of the quarks in the proton versus the radial distance r from the centre of the proton.
The thick black line corresponds to the pressure extracted from the D-term parameters fitted to published data measured at 6 GeV. The corresponding estimated uncertainties are displayed as the light-green shaded area shown. The blue area represents the uncertainties from all the data that were available before the 6-GeV experiment, and the red shaded area shows projected results from future experiments at 12 GeV that will be performed with the upgraded experimental apparatus.
Uncertainties represent one standard deviation.

So we will investigate the experimental result as for example a referee will do it

The experimental method: ❶ the data

Jlab 6 GeV With CLAS

21 bins in (x_B, Q^2) x 6 bins in t --- 3 months data taken in 2005

Girod et al. PRL100 (2008) 162002, Jo et al. PRL115, 212003 (2015)

$\overleftrightarrow{e} p \rightarrow e \gamma p$

$x_B \sim 2\xi/(1+\xi) \Rightarrow \xi \sim x_B/(2-x_B)$ $\quad |t|_{min} \sim m_p^2 x_B^2 / (1-x_B)$ if $x_B/Q \ll 1$

Bin 1	x_B =0.12	ξ=0.06	$\|t\|_{min}$=0.014
Bin 4-5	x_B =0.185	ξ=0.10	$\|t\|_{min}$=0.037
Bin 14-15	x_B =0.335	ξ=0.20	$\|t\|_{min}$=0.148
Bin 18-19	x_B =0.4	ξ=0.25	$\|t\|_{min}$=0.23

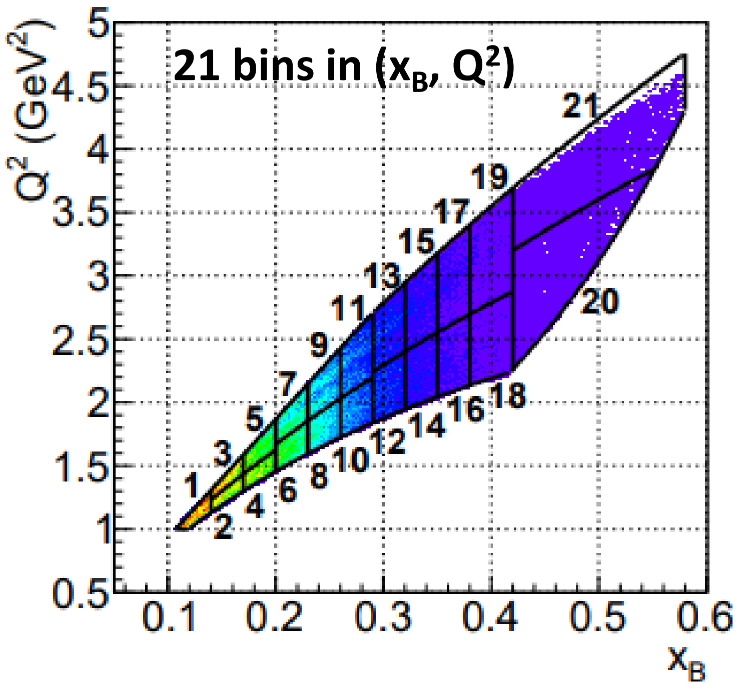

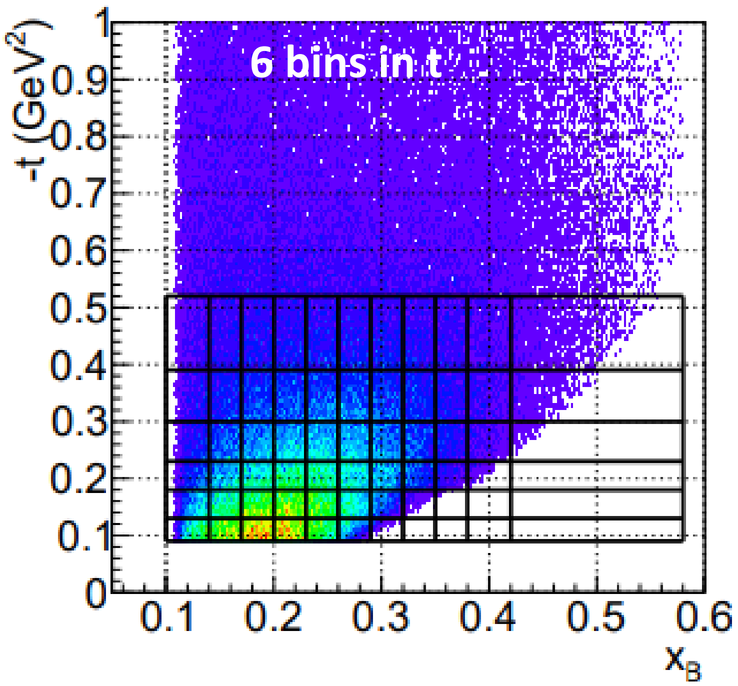

2005-2015: Beam Spin Sum and Diff of DVCS - CLAS

21 bins in (x_B, Q^2) or 110 bins (x_B, Q^2 t) 3 months data taken in 2005

Girod et al. PRL100 (2008) 162002, Jo et al. PRL115, 212003 (2015)

$\overleftrightarrow{e}\, p \rightarrow e\, \gamma\, p$

- **Re$\mathcal{H}$** for $\phi \sim \pi$
- **Im$\mathcal{H}$**

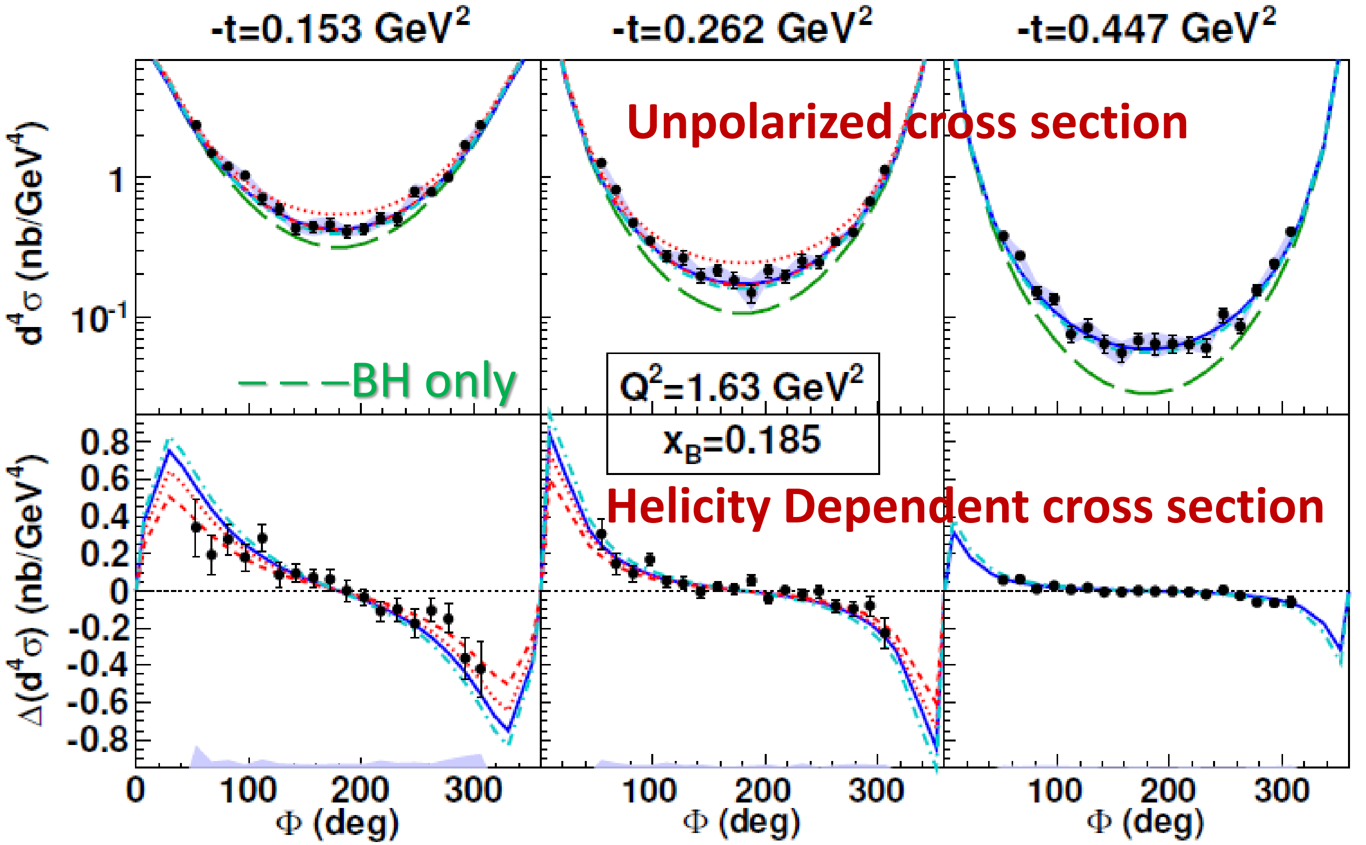

models:

VGG Vanderhaeghen, Guichon, Guidal PRL80(1998),PRD60(1999), PPNP47(2001), PRD72(2005)

1rst model of GPDs improved regularly

KMS12 Kroll, Moutarde, Sabatié, EPJC73 (2013)

using the **GK** model Goloskokov, Kroll, EPJC42,50,53,59,65,74

for GPD adjusted on the hard exclusive meson production at small x_B

"universality" of GPDs

KM10a – – – (KM10 ....) Kumericki, Mueller, NPB (2010) 841

Flexible parametrization of the GPDs based on both a Mellin-Barnes representation and dispersion integral which entangle skewness and t dependences

Global fit on the world data ranging from H1, ZEUS to HERMES, JLab

2005-2015: Beam Spin Sum and Diff of DVCS - CLAS

21 bins in (x_B, Q^2) or 110 bins (x_B, Q^2 t) 3 months data taken in 2005

Girod et al. PRL100 (2008) 162002, Jo et al. PRL115, 212003 (2015)

$\overleftrightarrow{e}\, p \rightarrow e\, \gamma\, p$

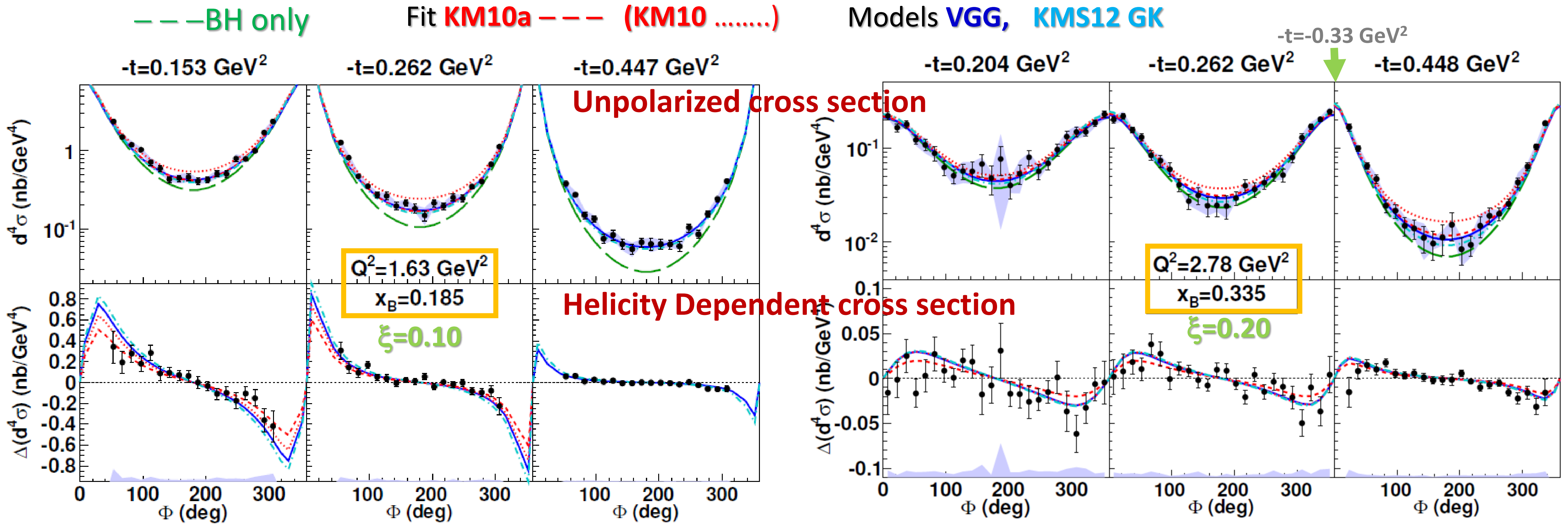

- The Beam Spin Difference presents a sinϕ evolution sensitive to **Im$\mathcal{H}$**
- The Beam Spin Sum is sensitive to DVCS2 or interference term or **Re$\mathcal{H}$** for ϕ around π where the statistics is weaker
- The statistics ↘ when $x_B \sim 2\xi$ ↗

The experimental method: ❷ Im$\mathcal{H}$ and Re$\mathcal{H}$ from local fits

In each (xb,t) bins extraction of **Im$\mathcal{H}$** and **Re$\mathcal{H}$**
according the formalism of Belitski, Mueller, Kirchner (Lecture II)

as HallA has done recently and carefully

today: Beam Spin Sum and Diff of DVCS - HallA @12GeV

E12-06-114 Hall-A experiment
in 2014-2016 with magnetic spectrometer

Georges et al., PRL128 (2022) 252002

Setting	Kin-36-1	Kin-36-2	Kin-36-3	Kin-48-1	Kin-48-2	Kin-48-3	Kin-48-4	Kin-60-1	Kin-60-3
x_B	0.36			0.48				0.60	
E_b (GeV)	7.38	8.52	10.59	4.49	8.85	8.85	10.99	8.52	10.59
Q^2 (GeV^2)	3.20	3.60	4.47	2.70	4.37	5.33	6.90	5.54	8.40
E_γ (GeV)	4.7	5.2	6.5	2.8	4.7	5.7	7.5	4.6	7.1
$-t_{min}$ (GeV^2)	0.16	0.17	0.17	0.32	0.34	0.35	0.36	0.66	0.70

Measurements for
3 high x_B=0.36, 0.48, 0.60
at 2 or 3 or 4 high Q^2 (or E_{beam})
in 3 or 5 bins in t
in 24 bins in φ.

Fit for constant (xB, t) using different beam energies (and Q^2) to separate DVCS^2, Interf. and BH

Formalism: Braun-Manashov-Müller-Pirnay, PRD 89, 074022 (2014)

ξ=0.22 x_B=0.36 x_B=0.48 x_B=0.60

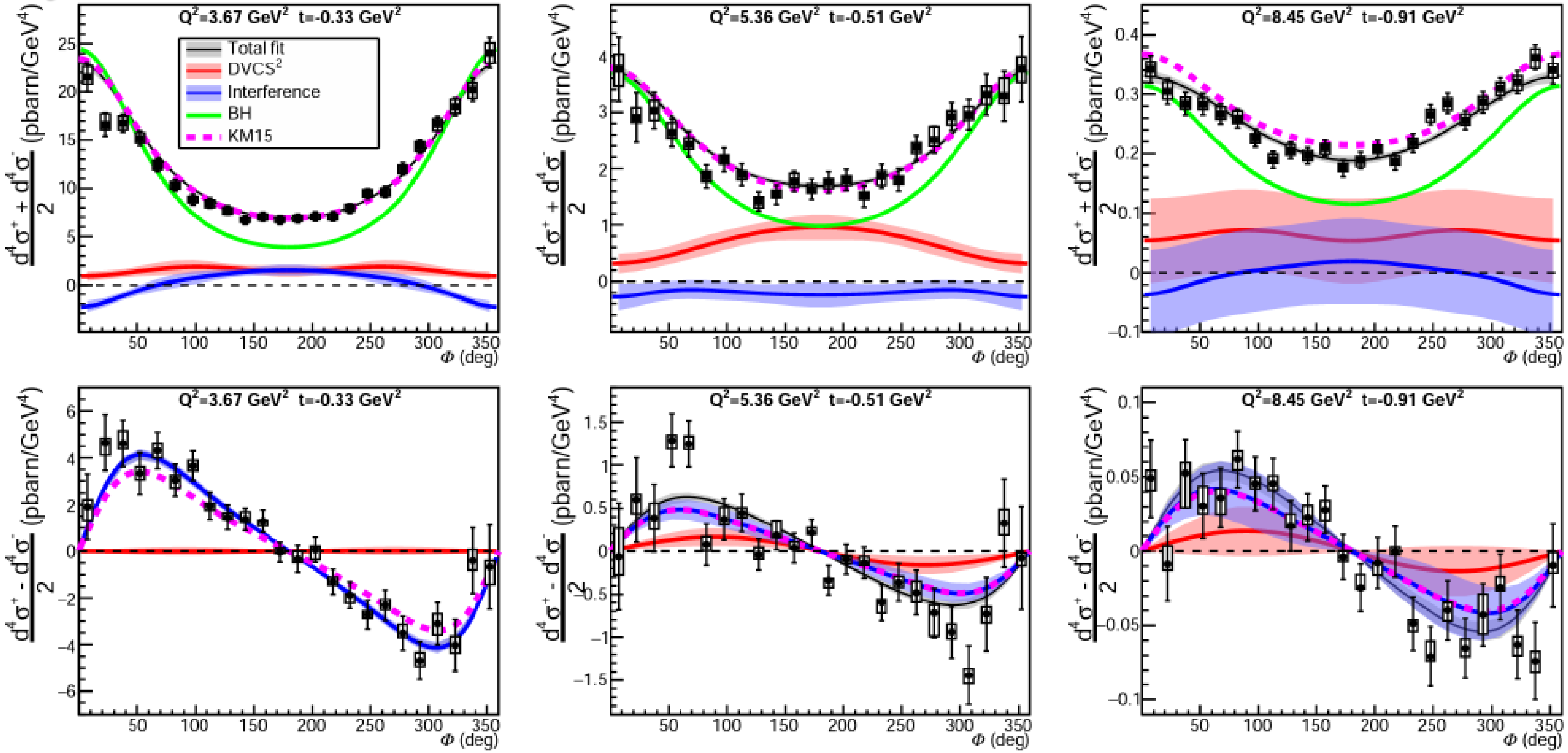

Prediction:

KM15: global fit of the world data

K. Kumericki and D. Mueller,
EPJ Web Conf. 112 (2016) 01012

today: Beam Spin Sum and Diff of DVCS - HallA @12GeV

Fit for constant (x_B, t) using different beam energies (but also different Q^2) of

- 24 CFF $(H, \tilde{H}, E, \tilde{E}) \otimes (\Re e, \Im m) \otimes (++, 0+, -+)$
- or only 8 CFF $(H, \tilde{H}, E, \tilde{E},) \otimes (\Re e, \Im m) \otimes (++)$

➔Importance of considering all CFFs when extracting helicity-conserving CFFs

Results for the better known CFFs H_{++} and $\tilde{H}_{++}$

x_B=0.6

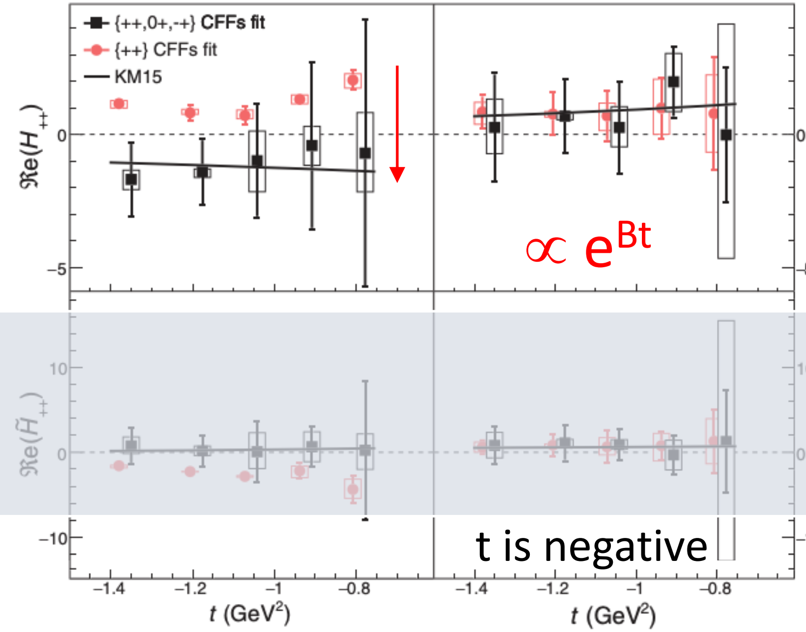

H_{++} and $\tilde{H}_{++}$ averaged over t

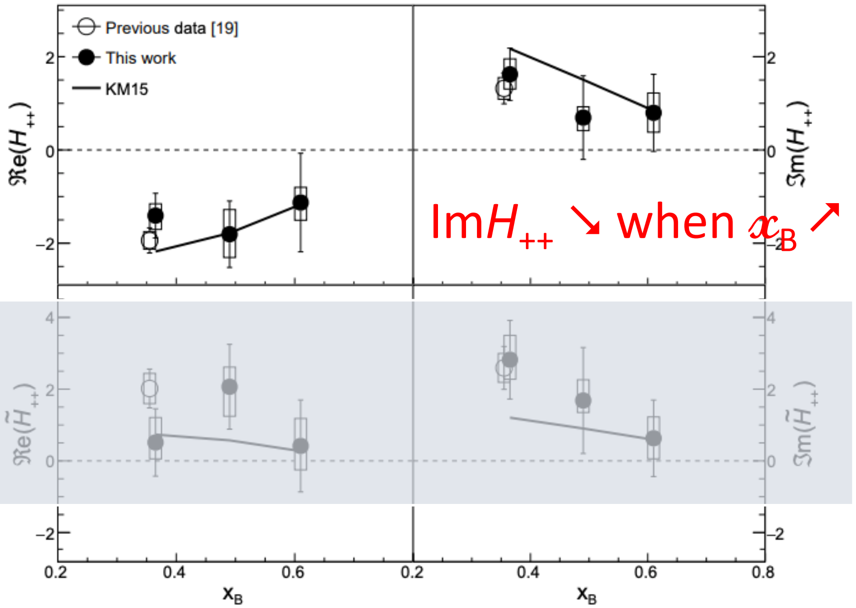

Georges et al., PRL128 (2022) 252002

<t>= −0.345, −0.702, −1.050 GeV² at x_B= 0.36, 0.48, 0.60

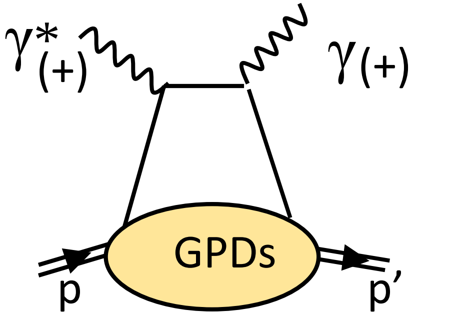

LO,Twist-2

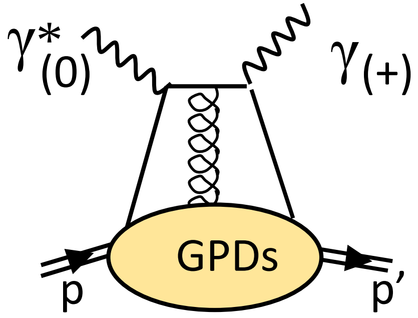

HT,Twist-3
suppressed by 1/Q

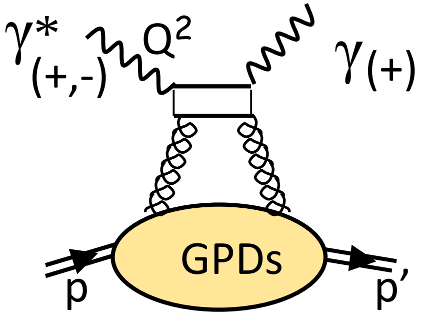

NLO,Twist-2
double helicity flip
suppressed by α_S

today: Beam Spin Sum and Diff of DVCS - HallA @12GeV

Fit for constant **(x_B, t)** using different beam energies (but also different Q^2) of

- ➢ 24 CFF $(H, \tilde{H}, E, \tilde{E}) \otimes (\Re e, \Im m) \otimes (++, 0+, -+)$
- ➢ or only 8 CFF $(H, \tilde{H}, E, \tilde{E},) \otimes (\Re e, \Im m) \otimes (++)$

➔ Importance of considering all CFFs when extracting helicity-conserving CFFs

Results for the better known CFFs H_{++} and $\tilde{H}_{++}$

x_B=0.6

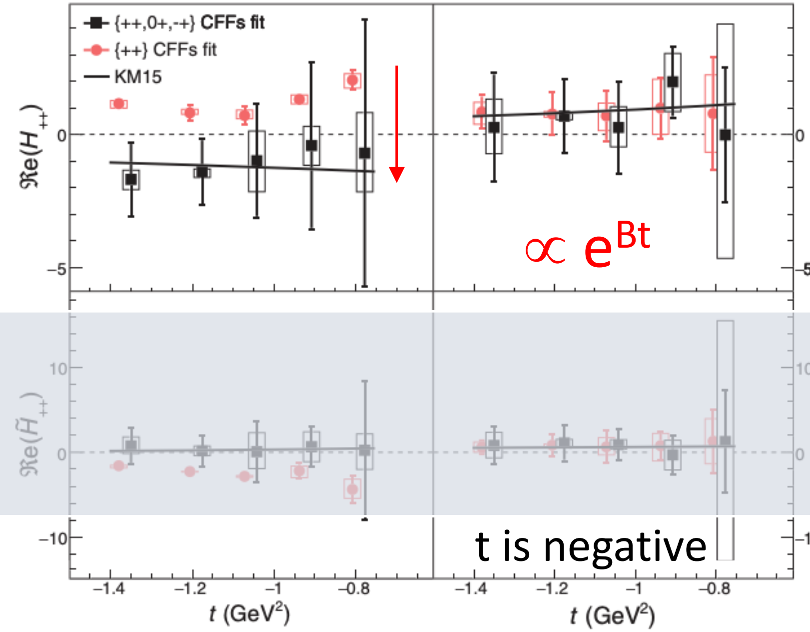

Georges et al., PRL128 (2022) 252002

x_B=0.36 ➔ ξ=0.22

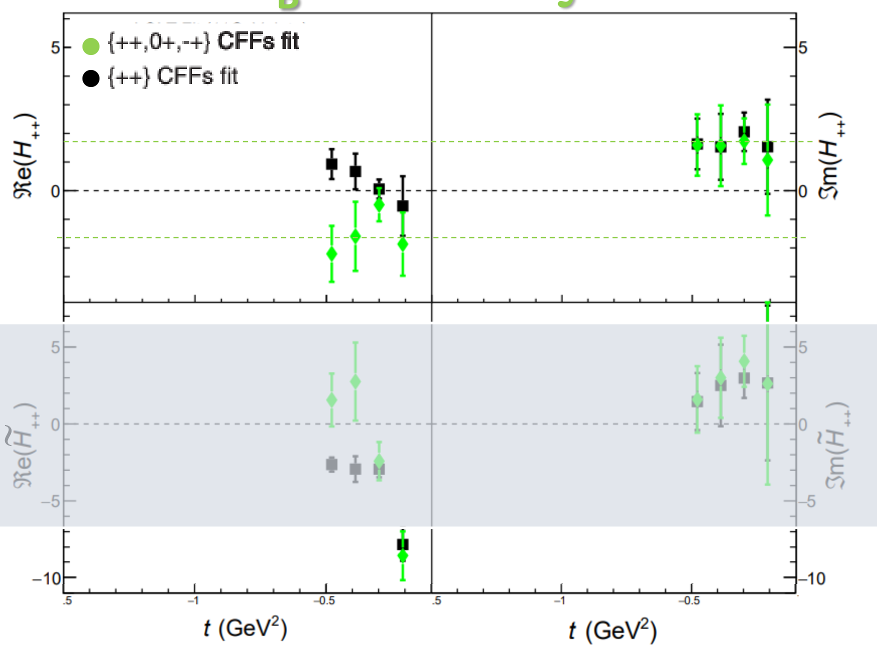

<t>= −0.345 GeV² |t|$_{min}$ >= 0.16 GeV²

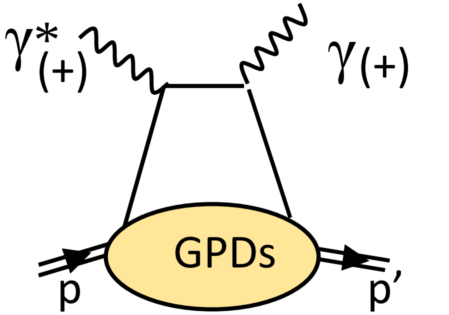

LO,Twist-2

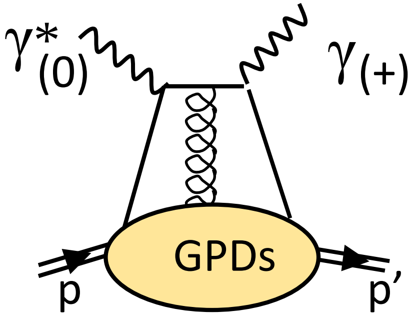

Twist-3
suppressed by 1/Q

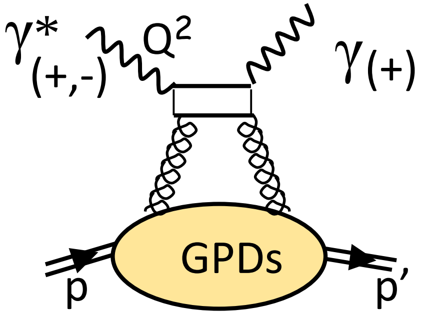

Twist-2, NLO
double helicity flip
suppressed by α_S

today: Beam Spin Sum and Diff of DVCS - HallA @12GeV

What do we learn?

- The Beam Spin Difference (or Asymmetry) presents a sinϕ evolution sensitive to **Im$\mathcal{H}$**

- The Beam Spin Sum is sensitive to DVCS2 or interference term or **Re$\mathcal{H}$** only in the ϕ domain around π where the statistics is weaker

- The statistics ↘ when $x_B \sim 2\xi$ ↗

- **Hall A has shown:**

  if Im$\mathcal{H}$ is relatively independent of HT and NLO
  this is not at all the case for **Re$\mathcal{H}$**

The experimental method: ❷ Im$\mathcal{H}$ and Re$\mathcal{H}$ from local fits

In each **(x_B,t)** bin ■ extraction of **Im$\mathcal{H}$** and **Re$\mathcal{H}$** according the formalism of Belitski, Mueller, Kirchner (Lecture II)

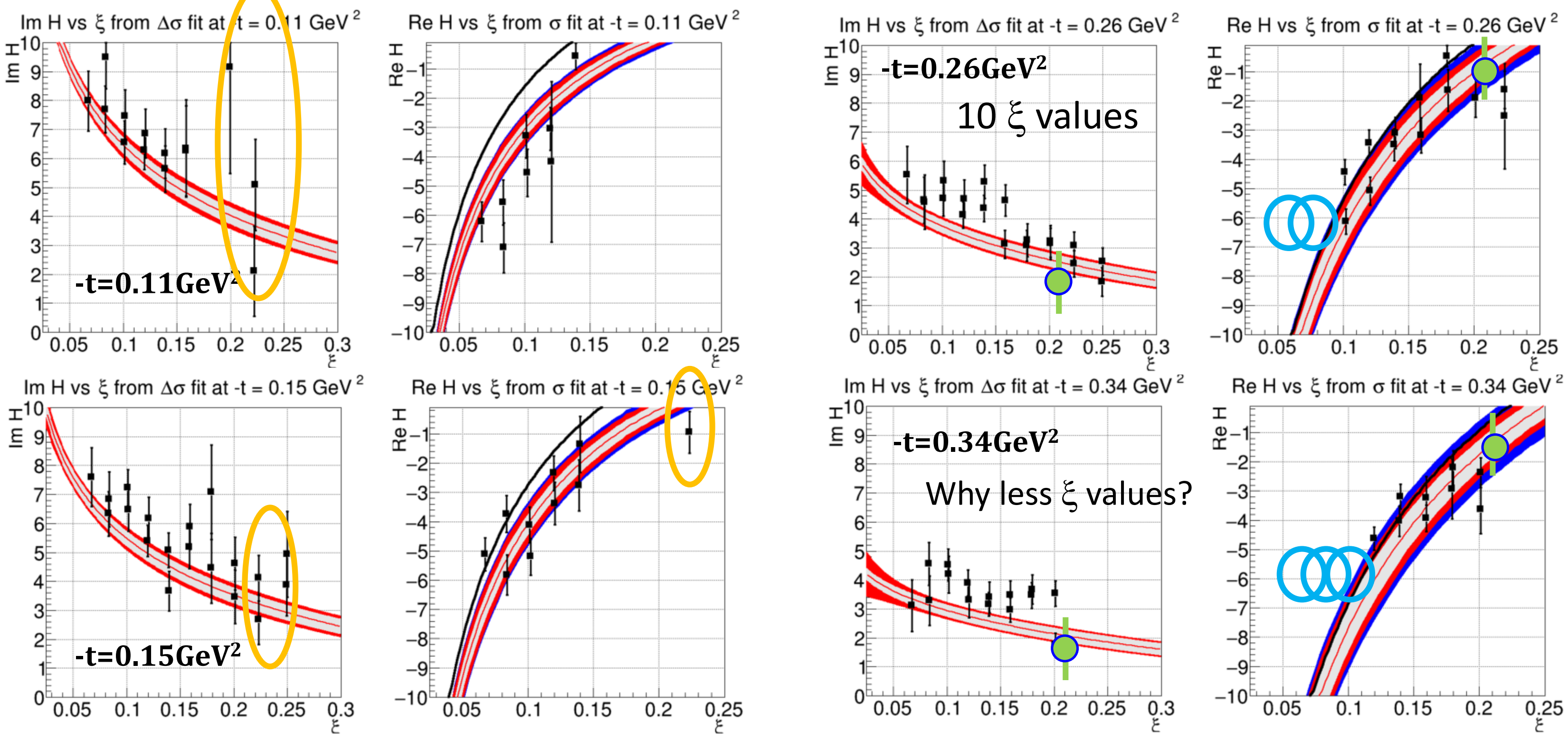

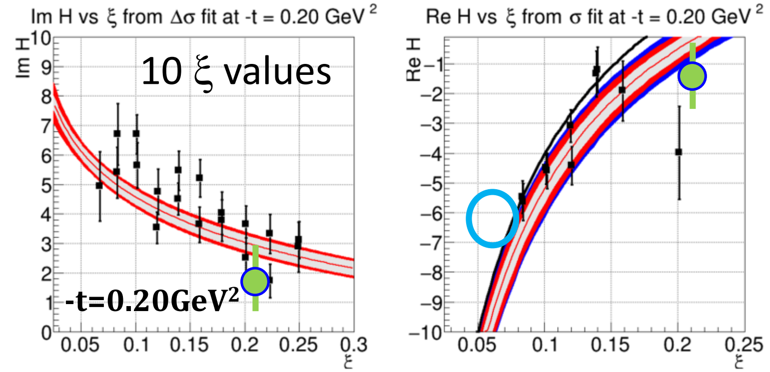

■ Jlab CLAS 6 GeV

The Real and Imaginary parts of Compton FF H(ξ,t) for different ξ and t values, resulting from the local fit to the **BSA** and **cross section data**.

Jlab HallA 12 GeV
In the domain of overlap

Important check as if **Im$\mathcal{H}$** is relatively independent of HT and NLO
this is not the case for **Re$\mathcal{H}$**

Data points for |t| < $|t|_{min}$?

No good statistics for **Re$\mathcal{H}$** determination at large |t| and small x_B

the Jlab 6 GeV CLAS data

Jlab 6 GeV With CLAS

21 bins in (x_B, Q^2) or 110 bins (x_B, Q^2 t) 3 months data taken in 2005

Girod et al. PRL100 (2008) 162002, Jo et al. PRL115, 212003 (2015)

$\overleftrightarrow{e}\, p \rightarrow e\, \gamma\, p$

$x_B \sim 2\xi/(1+\xi) \rightarrow \xi \sim x_B/(2-x_B)$ $|t|_{min} \sim m_p^2\, x_B^2/(1-x_B)$ if $x_B/Q \ll 1$

Bin 1	$x_B = 0.12$	$\xi=0.06$	$\lvert t\rvert_{min}=0.014$
Bin 4-5	$x_B = 0.185$	$\xi=0.10$	$\lvert t\rvert_{min}=0.037$
Bin 14-15	$x_B = 0.335$	$\xi=0.20$	$\lvert t\rvert_{min}=0.148$
Bin 18-19	$x_B = 0.4$	$\xi=0.25$	$\lvert t\rvert_{min}=0.23$

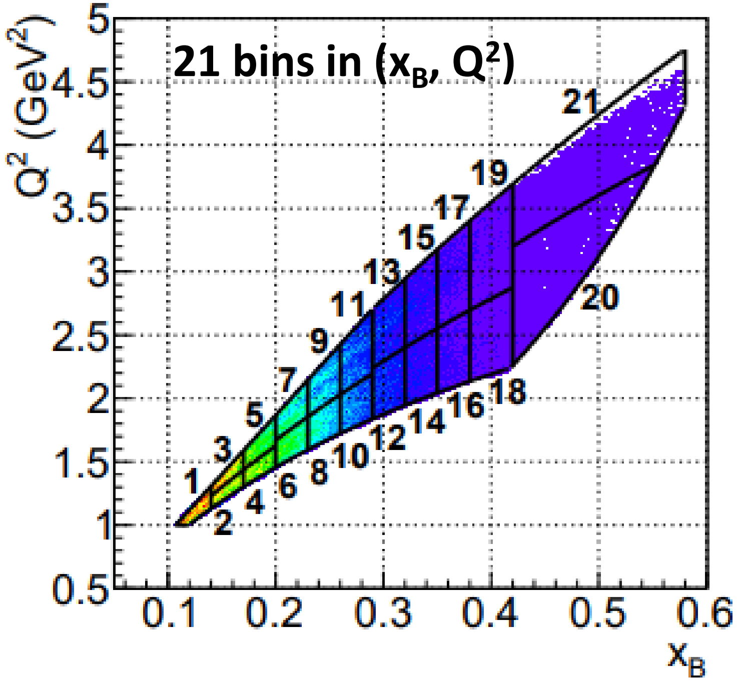

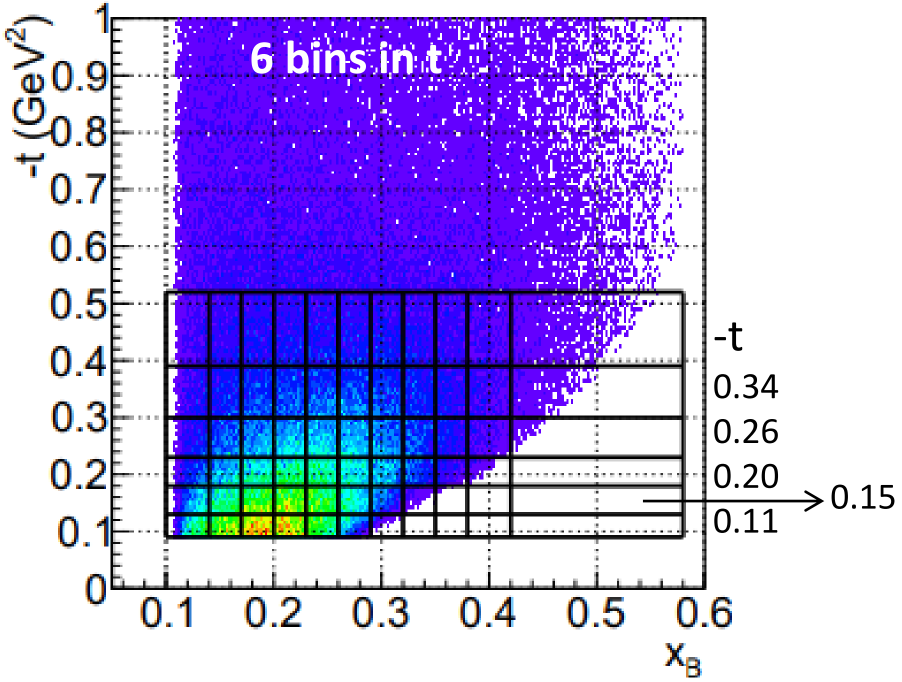

The experimental method: ❸ Im$\mathcal{H}$ and Re$\mathcal{H}$ from global fits

Global fit of ImH using the parametrisation from Kumericki and Mueller NPB841, 1-58, 2010

$$\mathrm{Im}\mathscr{H}(x,\ t) = \frac{nr}{1+x}\left(\frac{2x}{1+x}\right)^{-\alpha(t)}\left(\frac{1-x}{1+x}\right)^{b}\frac{1}{\left(1-\frac{1-x}{1+x}\frac{t}{M^2}\right)^{p}}$$

not completely valid at high t

Then ReH recontructed applying the DVCS dispersion relation with Δ(t) subtraction constant

$$\mathrm{Re}\mathscr{H}(\xi,\ t) = \Delta(t) + \frac{1}{\pi}\,\mathrm{P.V.}\int_0^1 dx\left(\frac{1}{\xi-x}-\frac{1}{\xi+x}\right)\mathrm{Im}\mathscr{H}(x,\ t)$$

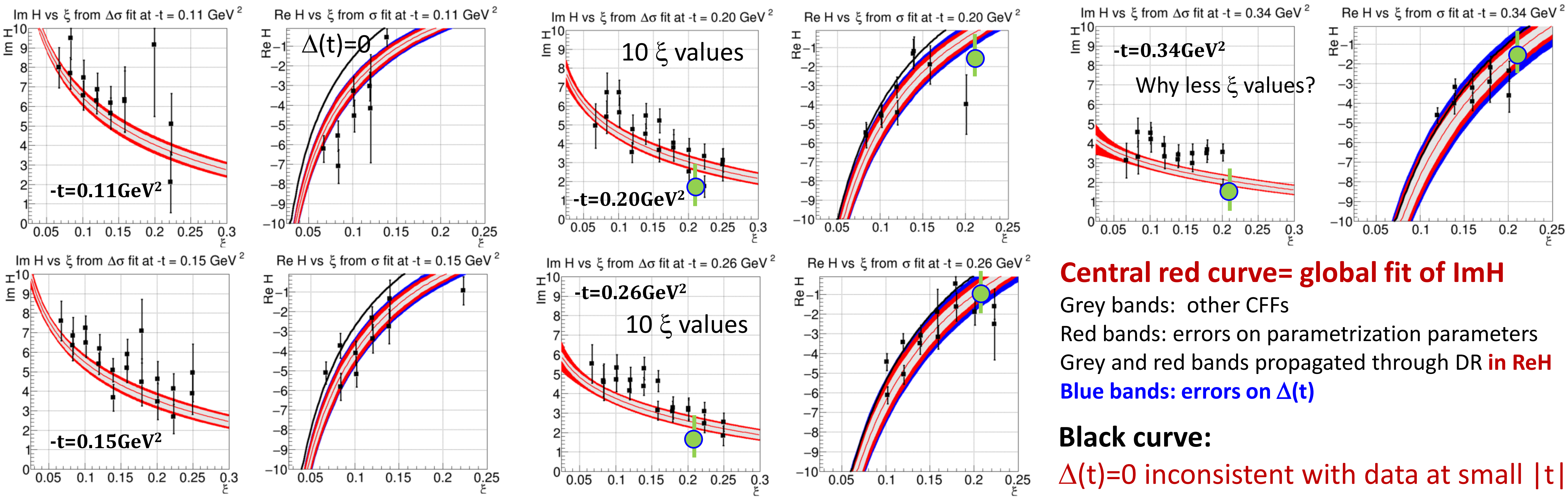

Central red curve= global fit of ImH

Grey bands: other CFFs

Red bands: errors on parametrization parameters

Grey and red bands propagated through DR **in ReH**

Blue bands: errors on Δ(t)

Black curve:

Δ(t)=0 inconsistent with data at small |t|

The experimental method: ❸ Im$\mathcal{H}$ and Re$\mathcal{H}$ from global fits

- Jlab CLAS 6 GeV

Samples of Beam Spin Asymmetry

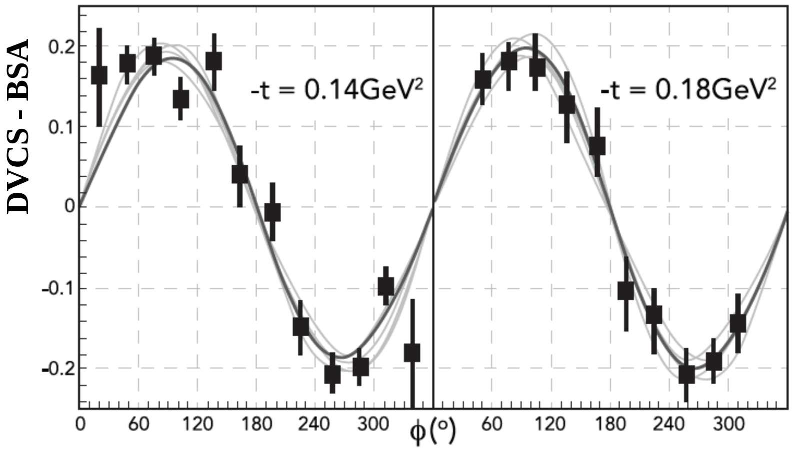

Thick grey curve: global fit of ImH
Thin light grey curves: errors on parametrization parameters within one standard deviation

Samples of differential cross sections with fits

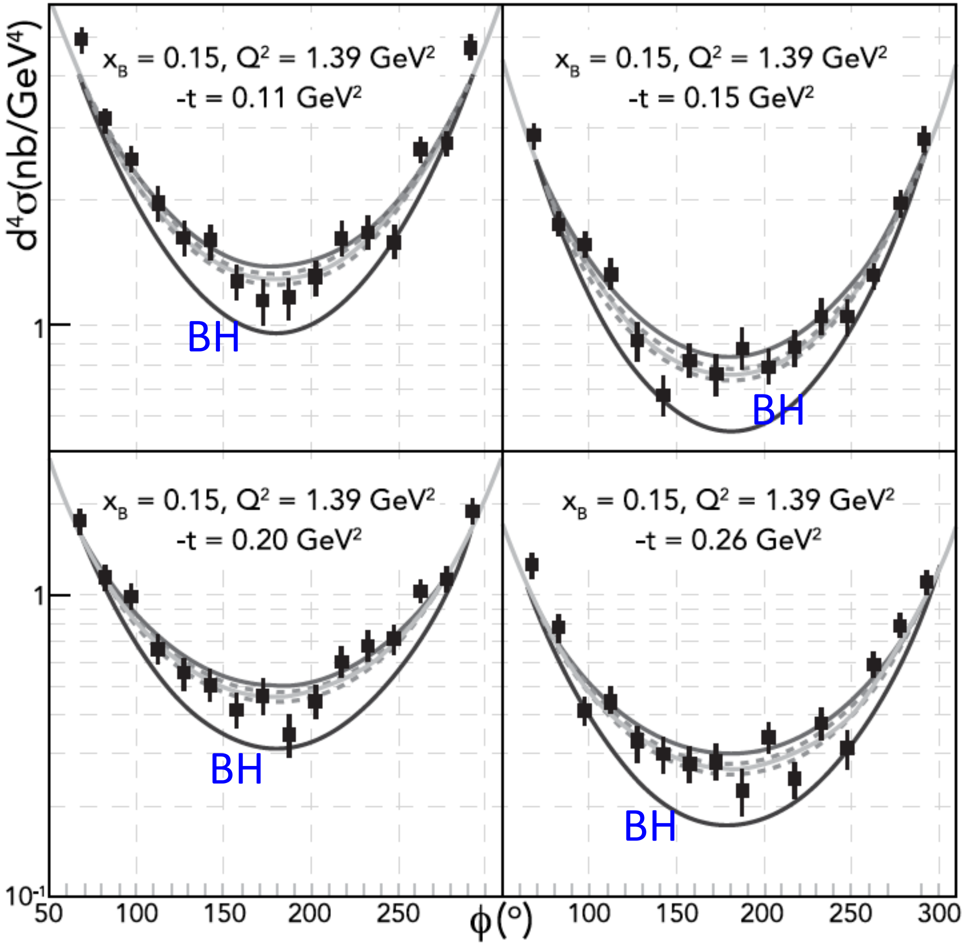

Thin light grey curves: local fit of ReH using the DR with $\Delta(t)$ at fixed t and variation within one standard deviation

Thick grey curve: global fit of ReH using the DR with a parametrization of $\Delta(t)$ $\Delta(t) = \Delta(0) \cdot (1-t/M^2)^{-\alpha}$

❹ Δ, D, d_1^q and Pressure distribution in the proton

Δ(t) subtraction constant of the DVCS dispersion relation:

$$\mathrm{Re}\mathscr{H}(\xi, t) = \Delta(t) + \frac{1}{\pi}\,\mathrm{P.V.}\int_0^1 dx \left(\frac{1}{\xi - x} - \frac{1}{\xi + x}\right)\mathrm{Im}\mathscr{H}(x, t)$$

Relation with D(z,t), the **D-term** of the GPD $\quad -1 < z = \frac{x}{\xi} < 1$

& with d_1^q(t), the **proton gravitational FF** (the spherical Bessel transform of the pressure):

$$\Delta(t) = 2\sum_q Q_q^2 \int_{-1}^{1} dz \frac{D_q(z,t)}{1-z} = 4\sum_q Q_q^2 \left(d_1^q(t) + \ldots\right), q = u, d, \ldots$$

next order terms <<

Q is the quark charge, considering only u and d quarks

And with the assumption $d_1^u = d_1^d = d_1^Q/2$

$$d_1^Q(t) = \frac{9}{10}\Delta(t)$$

The spherical Bessel transform of the pressure :

$$d_1(t) \propto \int d^3\mathbf{r}\, \frac{j_0(r\sqrt{-t})}{2t}\, p(r)$$

M.V. Polyakov, Phys. Lett. B555 (2003) 57

M.V. Polyakov, P. Schweitzer, Int.J.Mod.Phys. A33 (2018)

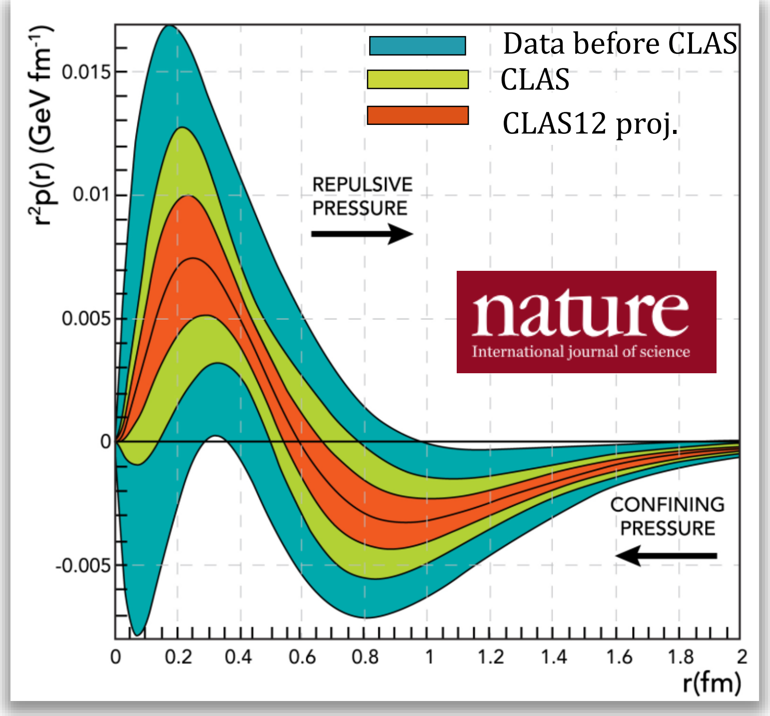

❹ Δ, D, d_1^q and Pressure distribution in the proton

With all the data for Beam Spin Diff and Sum of DVCS - CLAS@Jlab 6 GeV

$\overleftrightarrow{e}\, p \rightarrow e\, \gamma\, p$

Girod et al. PRL100 (2008) 162002, Jo et al. PRL115, 212003 (2015)

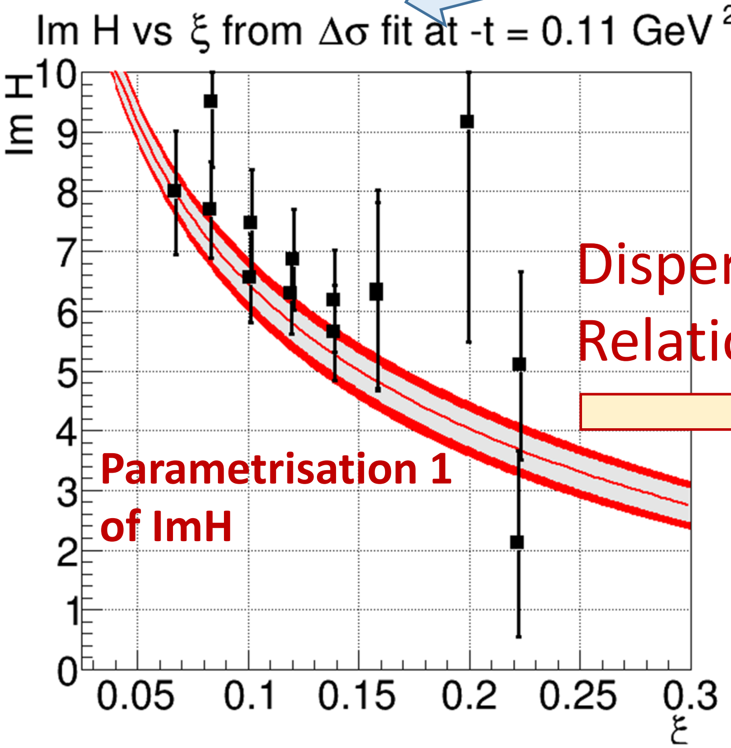

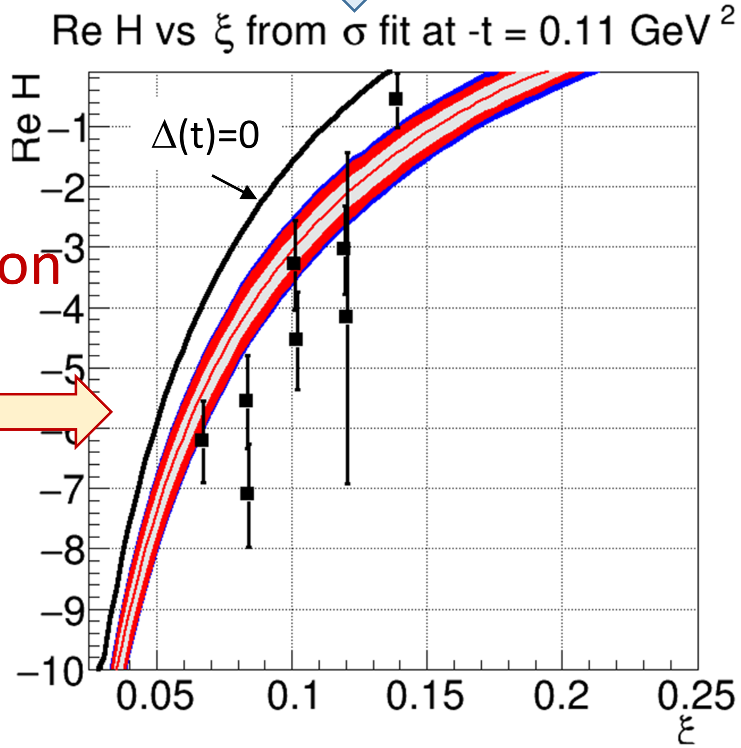

$d_1^Q(t) = 9/10\,\Delta(t)$

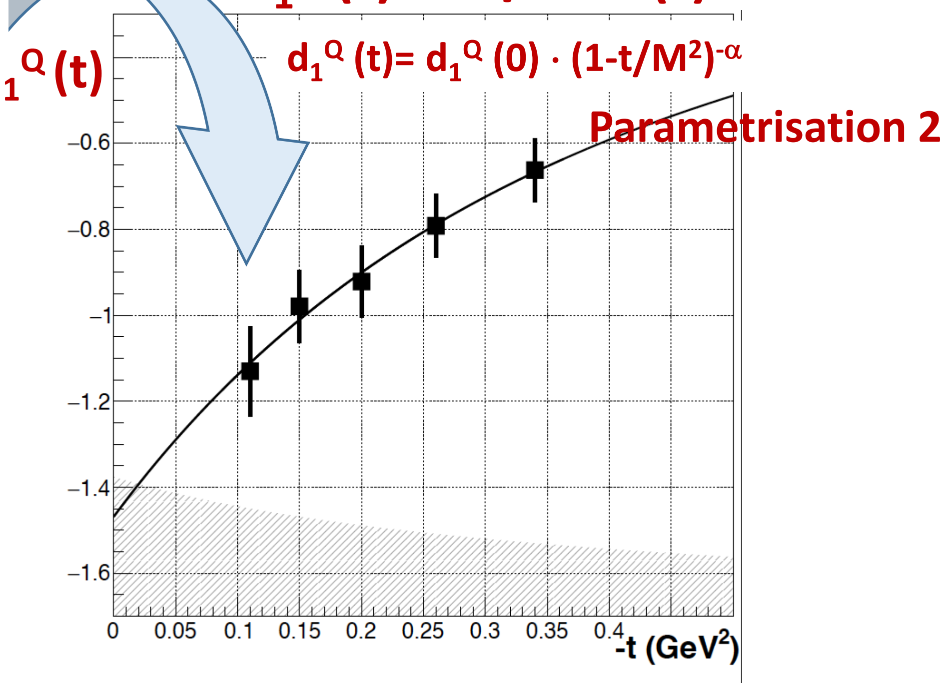

$d_1^Q(0) < 0$

This is a critical result, required for dynamical stability of the proton deeply rooted in chiral symmetry breaking.

$d_1^Q(0) = -1.47 \pm 0.10 \pm 0.22$

$M^2 = 1.06 \pm 0.10 \pm 0.15$

$\alpha = 2.76 \pm 0.25 \pm 0.50$

❹ Δ, D, d_1^q and Pressure distribution in the proton

Comparison of $d_1^Q(t)$ with theories

M. Polyakov, P. Schweitzer, Int.J.Mod.Phys. A33 (2018)

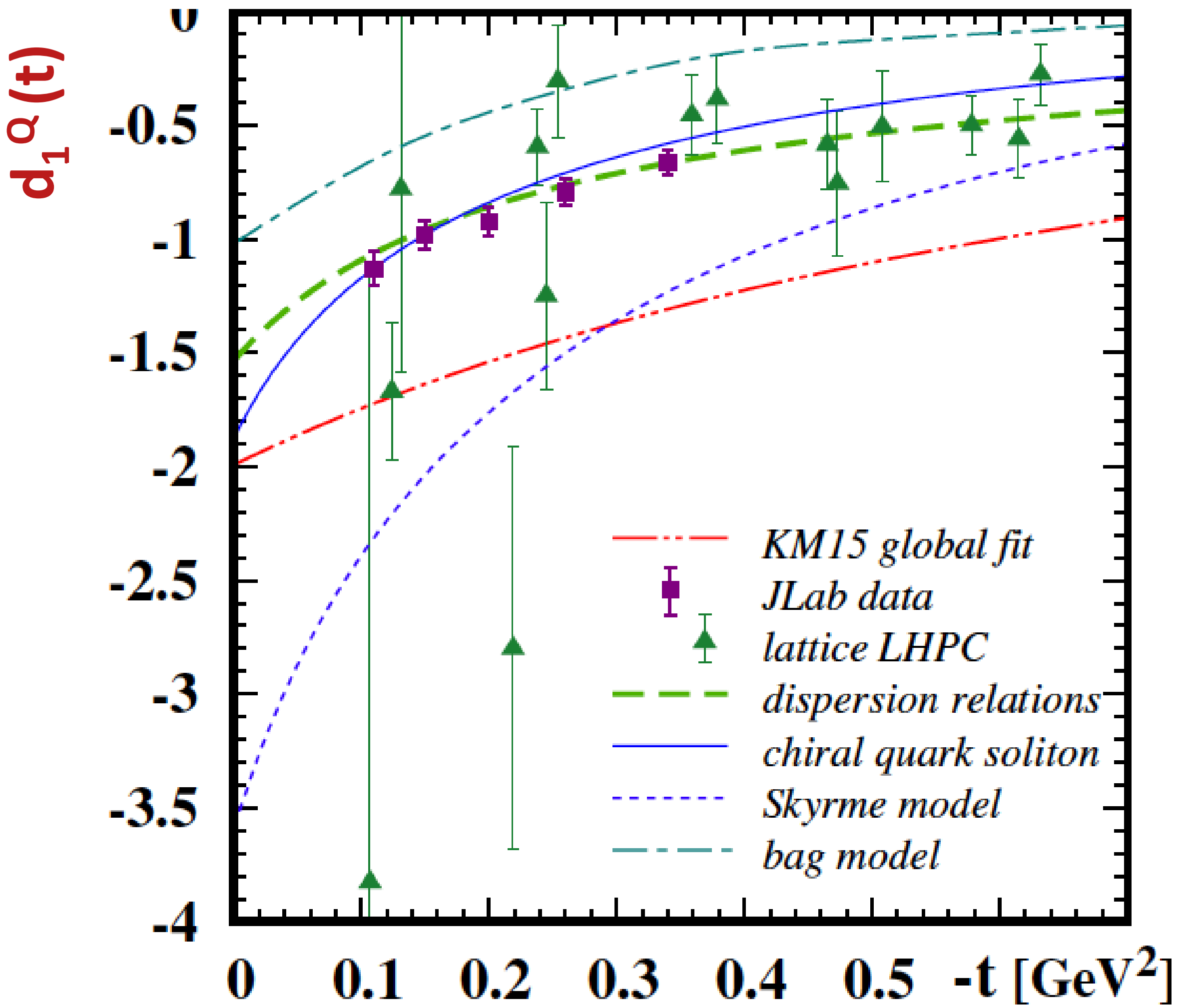

Global properties of the Proton

Em:	Q_{prot}	=	$1.602176487(40) \times 10^{-19}$C
	μ_{prot}	=	$2.792847356(23)\mu_N$
Weak:	g_A	=	$1.2694(28)$
	g_p	=	$8.06(0.55)$
Gravity:	M_{prot}	=	$938.272013(23)\,\mathrm{MeV}/c^2$
	J	=	$\frac{1}{2}$
	$d_1^Q(0)$	=	-1.47 (10) (22)

Pressure distribution and comparison to the χQSM model

In the chiral quark-soliton model (χQSM) the proton is modeled as a chiral soliton with the constituent quarks bound by a self-consistent pion field. The pion field provides the confining pressure at the proton periphery (pions are the Goldstone bosons of the spontaneous chiral symmetry breaking)

K. Goeke, M. Polyakov et al., Phys.Rev. D75 (2007)
M. Polyakov, P. Schweitzer, Int.J.Mod.Phys. A33 (2018)

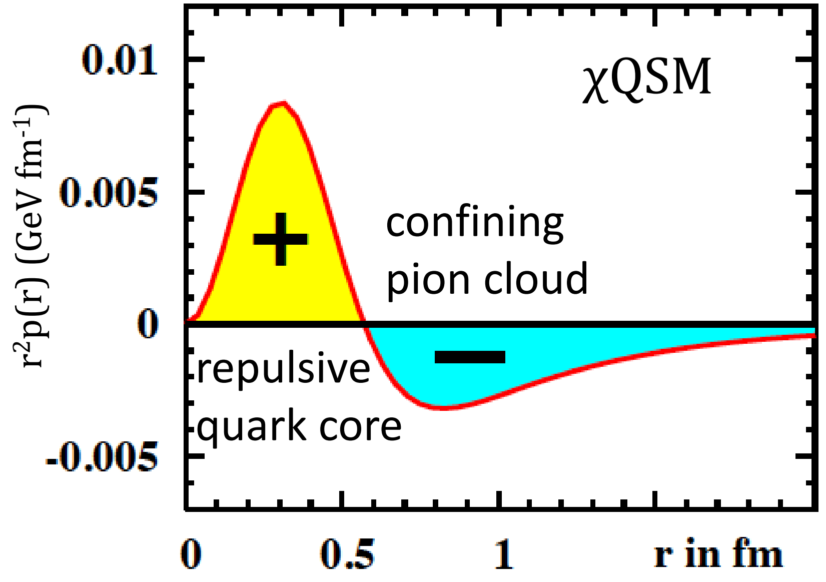

V.Burkert, L. Elouadrhiri, F.X. Girod
Nature 557 (2018) no.7705, 396-399

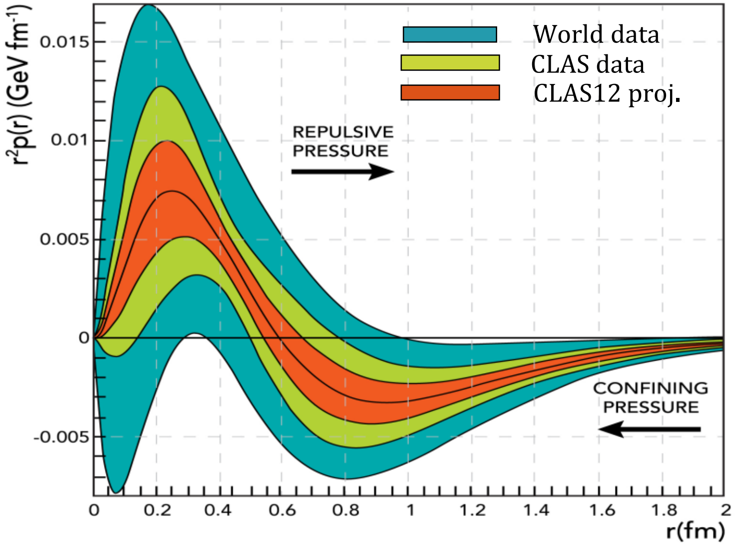

The $d_1^Q(0) < 0$ is rooted in the spontaneous chiral symmetry breaking (χSB).
In the χQSM the pion field provides the confining pressure at the proton's periphery.

BUT Problem of incertainties

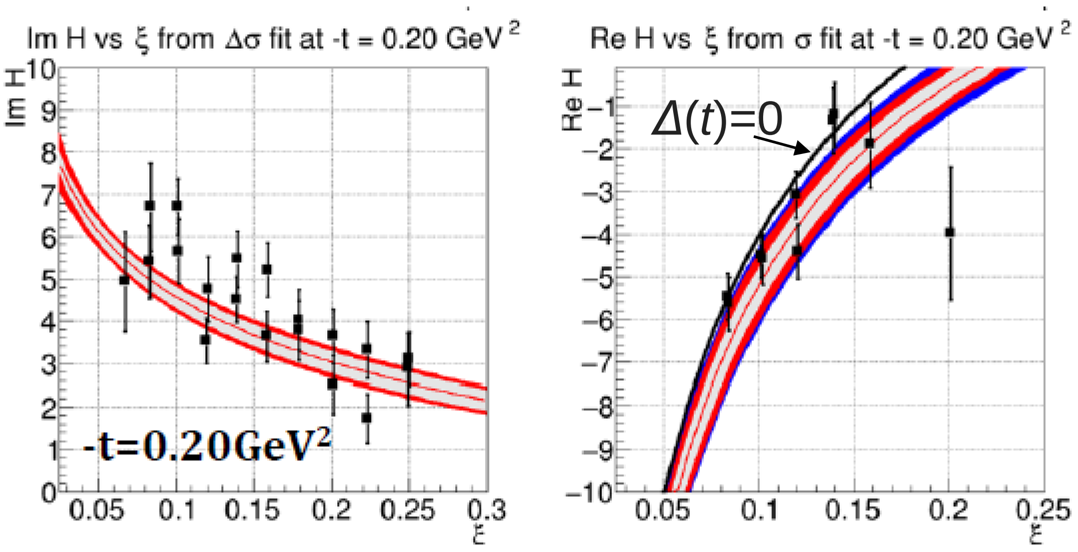

V. Burkert et al., Nature 557, 396-399 (**2018**)

nature International journal of science

acurate $\Delta(t)$ to determine D-term and pressure

within some assumptions

$\Delta(t=0)$ = -1.63 ± 0.11 ± 0.24 $d_1^Q = 9/10\ \Delta(t)$

This is a critical result,
required for dynamical stability of the proton,
deeply rooted in chiral symmetry breaking.

however improvement of uncertainties

Using flexible parametrization by neural networks

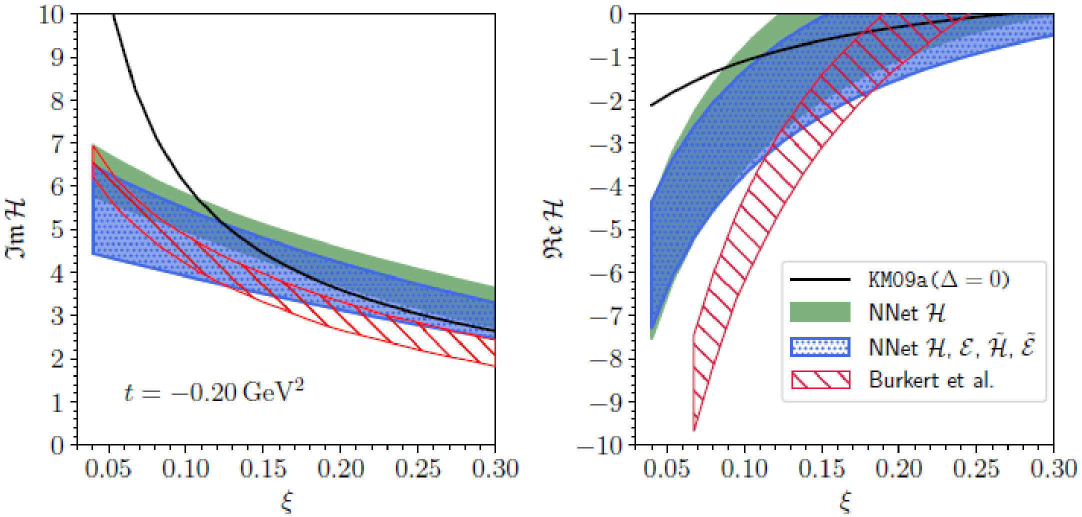

By Kumericki: Fits à la Burkert, by applying NNet to the CLAS DVCS data, as well as by the fit of KM09a) with zero subtraction constant. Coloured bands for uncertainty of one standard deviation.

K. Kumericki, Nature 570, E1–E2 (**2019**)

$\Delta(t)$ = 0.78 ± 1.5 (statistical uncertainty)

with almost no dependence on t

➔ D-term and pressure consistent with 0

➔ waiting for more data sensitive to **ReH**

(importance of DVCS with $\mu^\pm$ at COMPASS, $e^\pm$ at JLab or TCS at JLab and EIC)

ImH and ReH using global fits of the world data

Global Fit KM15
Compared to GK Model GK
Kumericki, Mueller, NPB (2010) 841, private com.

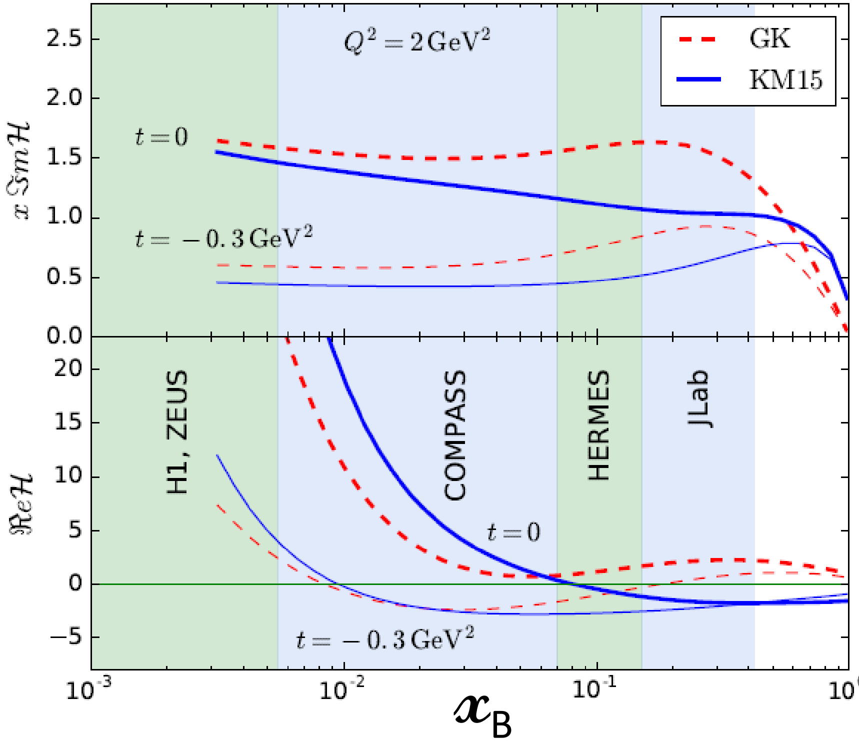

Global Fits using PARTONS framework
Compared to GK and VGG Models
Moutarde, Sznajder, Wagner, Eur. Phys. J. C 79 (2019) 7, 614

PARTONS: global Fit
PARTONS: Neural Network
to reduce the model dependency
...... GK
---- VGG

for $t = -0.3\,\mathrm{GeV}^2$ and $Q^2 = 2\,\mathrm{GeV}^2$

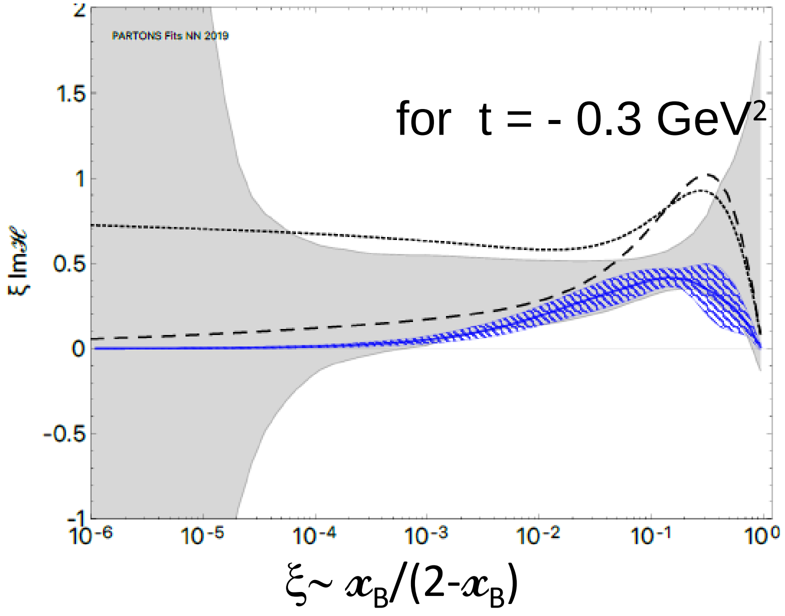

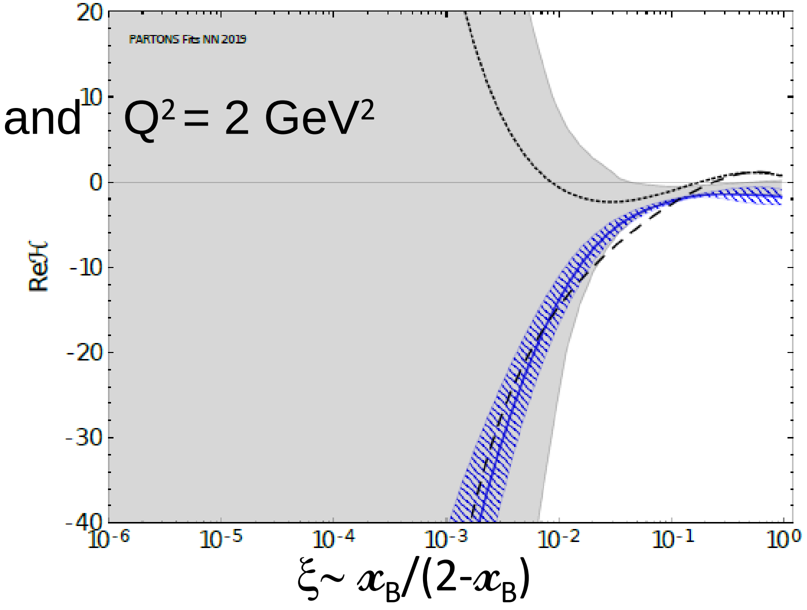

ReH is still poorly known (importance of DVCS with $\mu^{\pm}$ at COMPASS, $e^{\pm}$ at JLab or TCS at JLab and EIC)

Incertainties on the subtraction term $C_H(t,Q^2)$

$$\Delta(t) = \mathcal{C}_H(t,Q^2) = \mathrm{Re}\,\mathcal{H}(\xi,t,Q^2) - \frac{1}{\pi}\int_0^1 d\xi'\,\mathrm{Im}\,\mathcal{H}(\xi',t,Q^2)\left(\frac{1}{\xi-\xi'} - \frac{1}{\xi+\xi'}\right)$$

PARTONS: Neural network
Moutarde, Sznajder, Wagner,
Eur. Phys. J. C 79 (2019) 7, 614

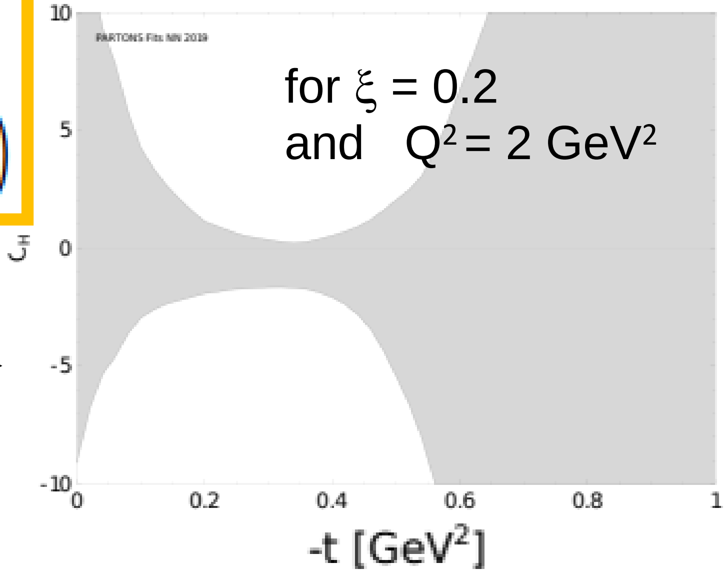

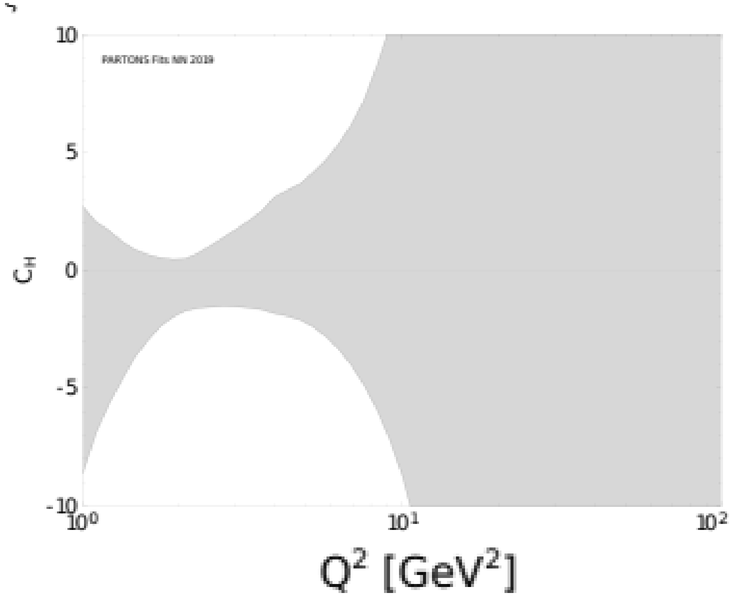

Incertainties on the subtraction term $C_H(t,Q^2)$

$$\mathcal{C}_H(t,Q^2) = \mathrm{Re}\,\mathcal{H}(\xi,t,Q^2) - \frac{1}{\pi}\int_0^1 \mathrm{d}\xi'\,\mathrm{Im}\,\mathcal{H}(\xi',t,Q^2)\left(\frac{1}{\xi-\xi'} - \frac{1}{\xi+\xi'}\right)$$

PARTONS: Neural network →

Moutarde, Sznajder, Wagner,
Eur. Phys. J. C 79 (2019) 7, 614

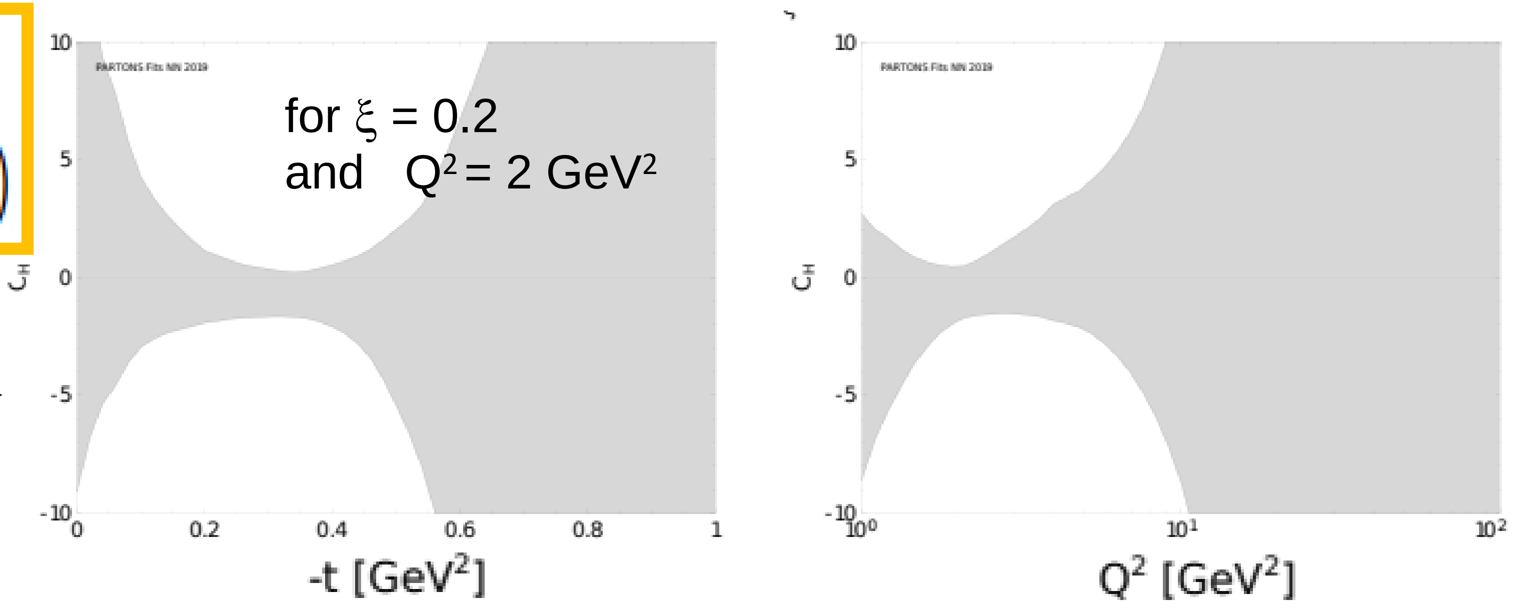

with the ansatz →

$$d(t,\mu_F^2) = d(\mu_F^2)\left(1 - \frac{t}{\Lambda^2}\right)^{-\alpha}$$

$$d \in \{d_1^{uds}, d_3^{uds}, d_1^c, d_1^g\}$$

$\Lambda = 0.8$ GeV and $\alpha = 3$ are kept fixed

Dutrieux, Moutarde et al.,
Eur. Phys. J. C 81 (2021) 300

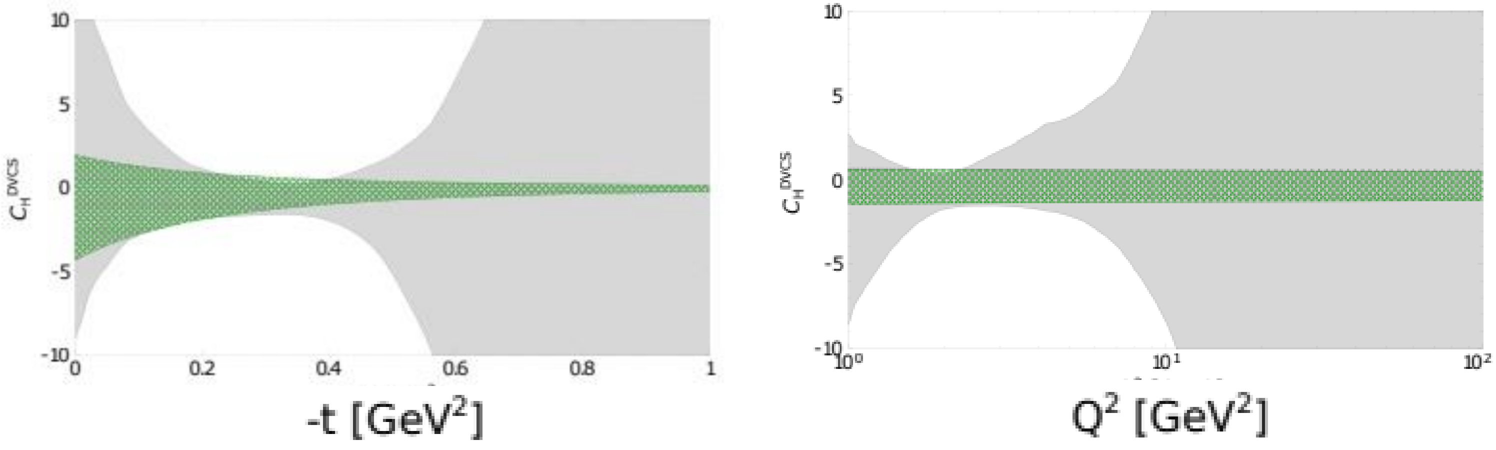

CONCLUSION

The link between the distribution of pressure forces in the proton and the DVCS subtraction constant is well-defined.

DVCS data do not allow yet a statistically significant extraction of these pressure forces.

We need more precise data and an extension of the covered kinematic domain.
We need to reach small t values

→ Role of the future experiments at JLab, CERN, EIC and EIcC facilities.

next future: DVCS with Beam Spin Sum and Diff @ JLab12

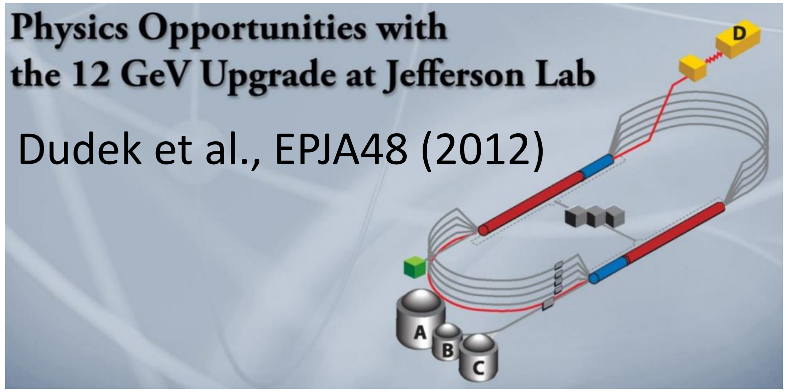

Projection for Jlab 12 GeV

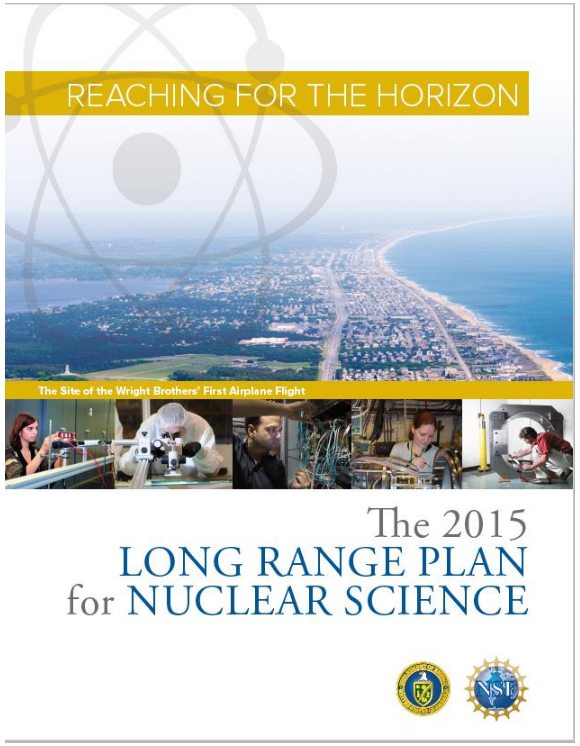

Transverse profile

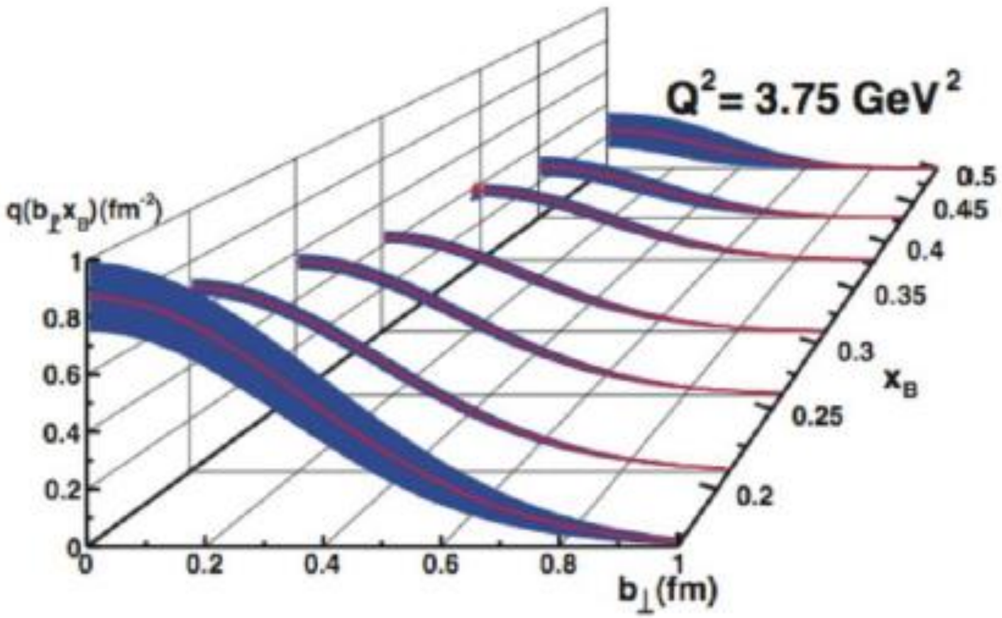

Pressure Distribution

E12-06-119
E12-16-010

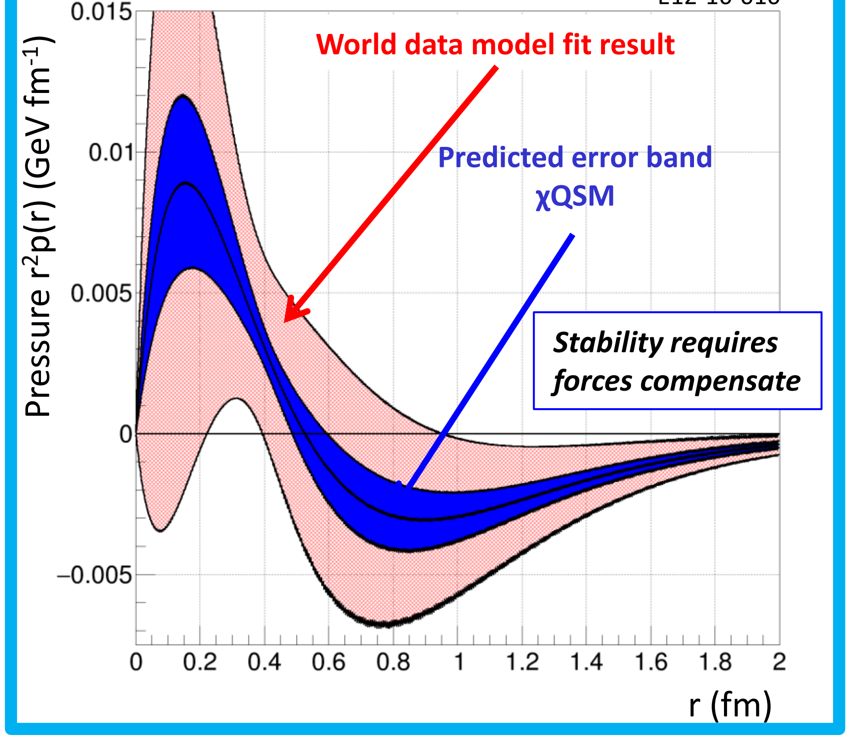

Future: Physics Program at EIC and Detector Projet

arXiv:1212.1701.v3
Eur. Phy. J. A 52, 9 (2016)

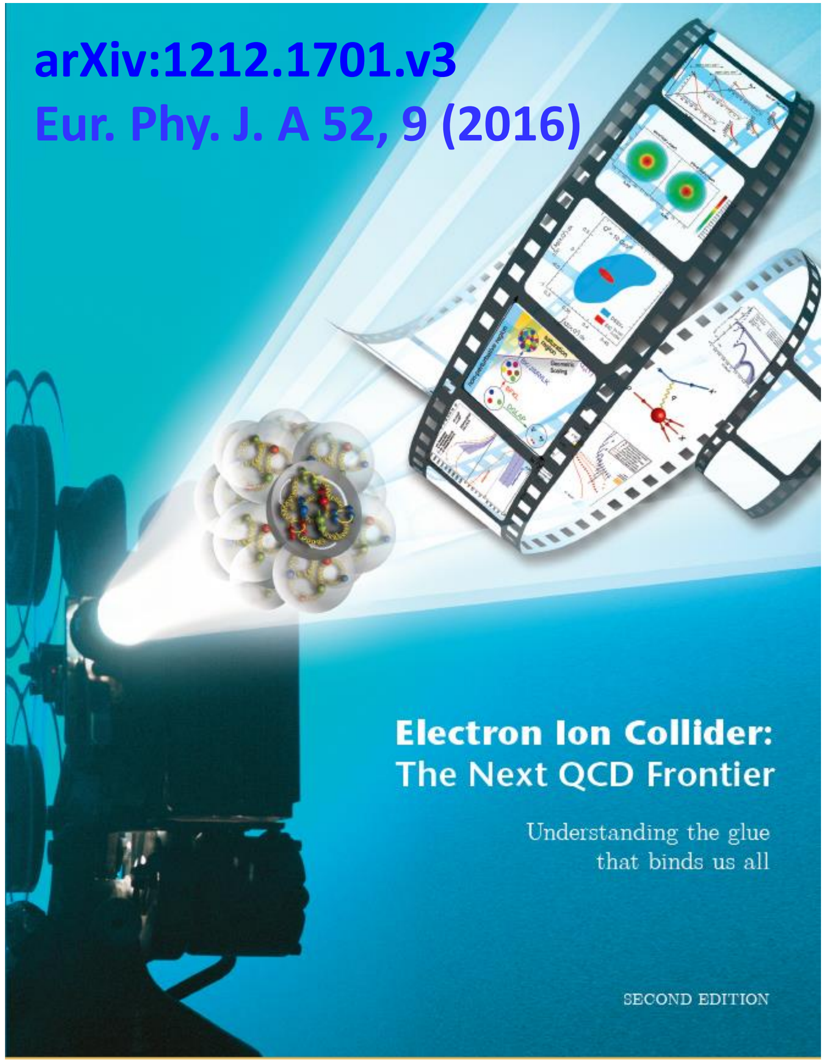

arXiv:2103.05419

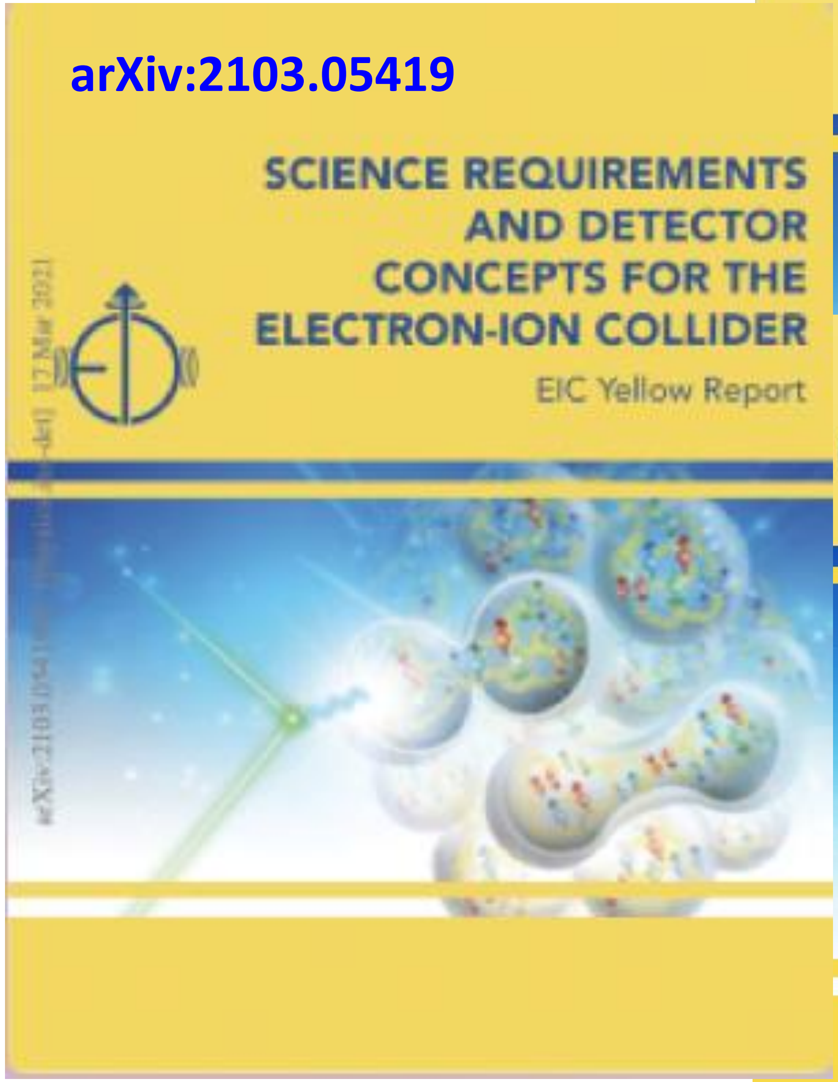

Future: Physics Program at EIC and Detector Projet

DOE annoncement: January 9, 2020
CD0 December 19, **2019**
Site of EIC: Brookhaven National Laboratory

BNL and Jlab realize EIC as partners
CD1 June 28, **2021**

CD2 Approval - Early FY24

CD3 Start of construction - Early FY25

CD4A early finish, collisions begin for machine tuning
Detector 1 needs to be ready to give feedback. – FY31

CD4 Machine delivers for physics
Detector 1 should be fully functional to start physics –FY33


Y.GOV SCIENCE & INNOVATION ENERGY ECONOMY SECURITY & SAFETY SAVE ENERGY, MONEY

Department of Energy

U.S. Department of Energy Selects Brookhaven National Laboratory to Host Major New Nuclear Physics Facility

JANUARY 9, 2020

Home » U.S. Department of Energy Selects Brookhaven National Laboratory to Host Major New Nuclear Physics Facility

WASHINGTON, D.C. – Today, the **U.S. Department of Energy (DOE)** announced the selection of Brookhaven National Laboratory in Upton, NY, as the site for a planned major new nuclear physics research facility.

EIC physics at-a-glance

Understanding the glue that binds as all

How are the sea quarks and gluons, and their spins, distributed in space and momentum inside the nucleon?
How do the nucleon properties (mass & spin) emerge from their interactions?

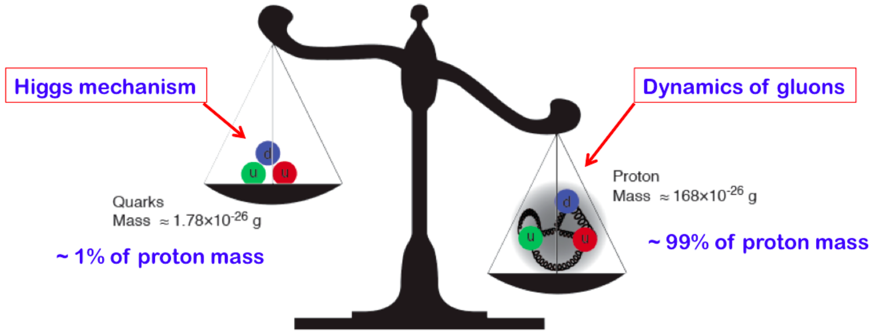

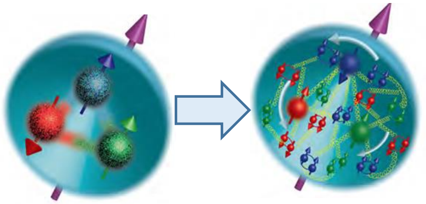

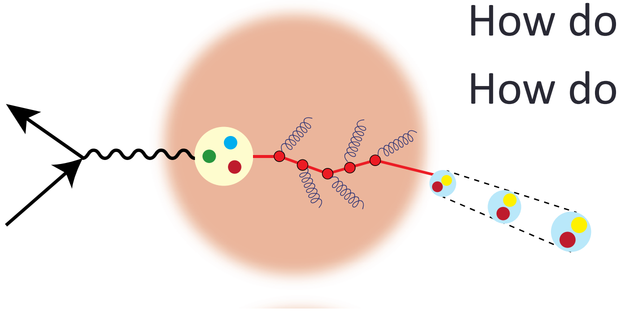

How do color-charged quarks and gluons and colorless jets, interact with a nuclear medium?
How do the confined hadronic states emerge from these quarks and gluons?
How do the quark-gluon interactions create nuclear binding?

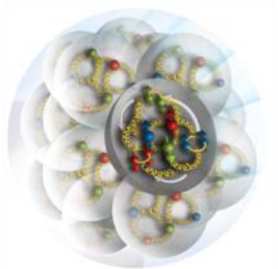

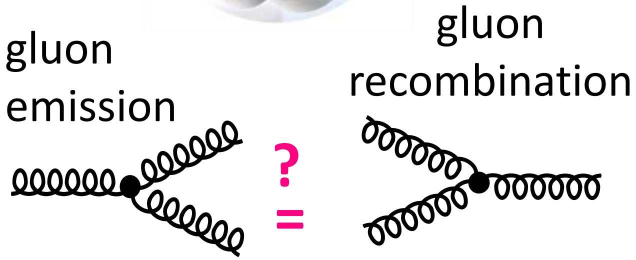

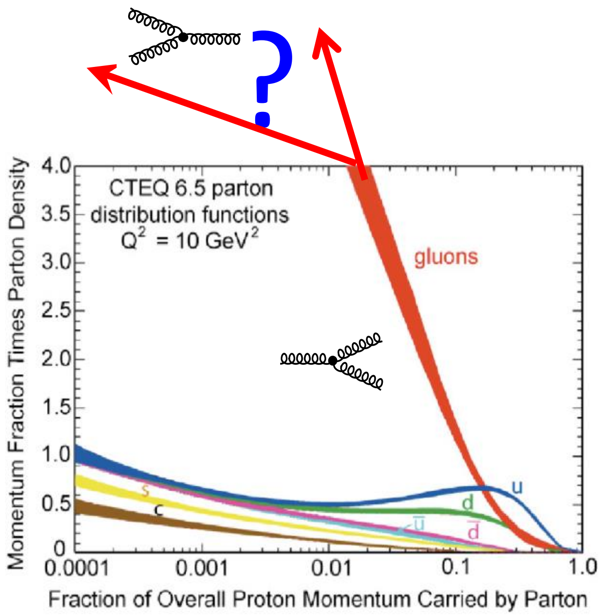

How does a dense nuclear environment affect the quarks and gluons, their correlations, and their interactions?
What happens to the gluon density in nuclei? Does it saturate at high energy, giving rise to a gluonic matter with universal properties in all nuclei, even the proton?

EIC project at BNL

Ee (GeV)	Ep (GeV)	√s (GeV)
5	41	29
5	100	45
10	100	63
18	275	141

p: 41 GeV, 100 to 275 GeV — p/A beam →

← e beam — e: 5 GeV to 18 GeV

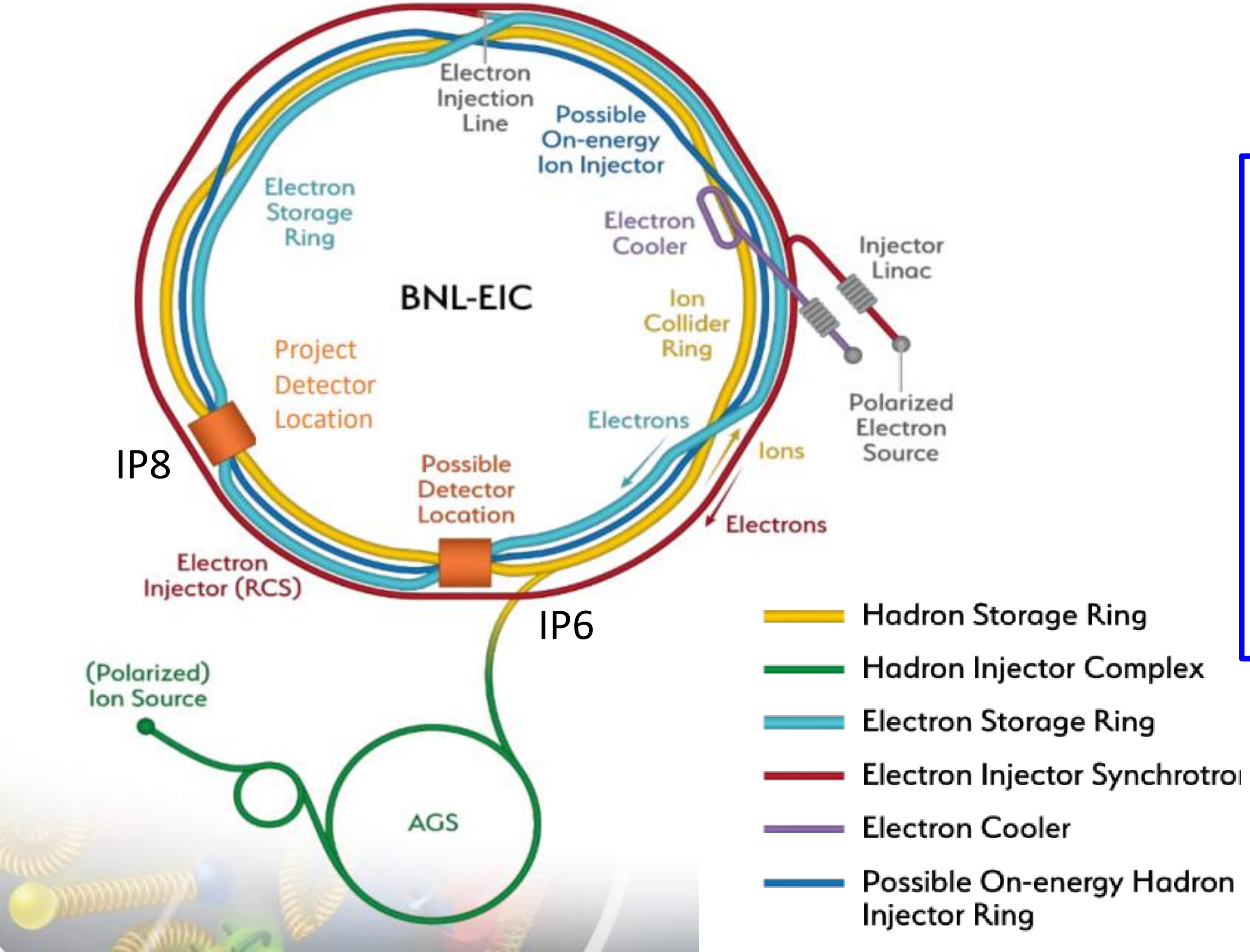

Project Design Goals

- High Luminosity: L= $10^{33} – 10^{34}$ $cm^{-2}sec^{-1}$, 10 – 100 fb^{-1}/year
- Highly Polarized Beams: 70%
- Large Center of Mass Energy Range: E_{cm} = 29 – 140 GeV
- Large Ion Species Range: protons – Uranium
- Large Detector Acceptance and Good Background Conditions
- Accommodate a Second Interaction Region (IR)

IP6 equipped with a 1st detector for 2032
IP8 equipped with a 2nd detector
in 2-5 years later

Key measurements for gluon imaging with EIC

Stage 2
Ee=20 GeVEp=250 GeV

Stage 1
Ee=5 GeVEp=100 GeV

Deliverables	Observables	What we learn	Requirements
GPDs of sea quarks and gluons	DVCS and $J/\Psi, \rho^0, \phi$ production cross section and polarization asymmetries	transverse spatial distrib. of sea quarks and gluons; total angular momentum and spin-orbit correlations	$\int dt\, L \sim 10$ to $100\,\mathrm{fb}^{-1}$; Roman Pots; polarized e^- and p beams; wide range of x_B and Q^2; range of beam energies; e^+ beam valuable for DVCS
GPDs of valence and sea quarks	electroproduction of π^+, K and ρ^+, K^*	dependence on quark flavor and polarization	

DVCS, TCS
Exclusive production of J/ψ and Υ

3D imaging – gluon distribution from low to high x

exclusive J/ψ production at EIC

mapping in the transverse plane
Impact parameter distribution

$$q_f(x, b_\perp) = \int \frac{d^2\Delta_\perp}{(2\pi)^2} e^{-i\Delta_\perp \cdot b_\perp} H_f(x, 0, -\Delta_\perp^2)$$

$$\langle b_\perp^2 \rangle^q(x) = -4 \frac{\partial}{\partial \boldsymbol{\Delta}_\perp^2} \ln H_-^q(x, 0, -\boldsymbol{\Delta}_\perp{}^2)\Big|_{\boldsymbol{\Delta}_\perp = 0}$$

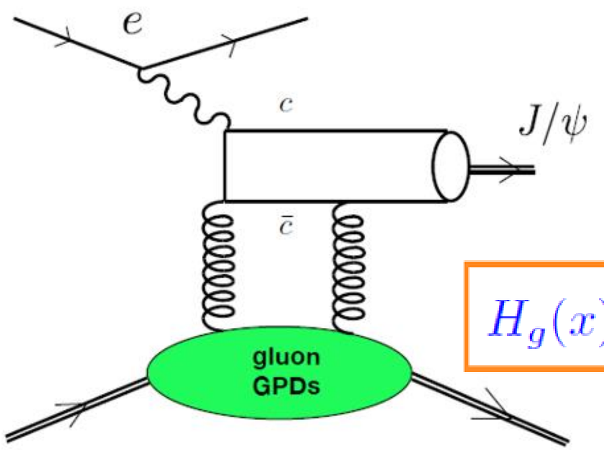

$$H_g(x), E_g(x)$$

Exclusive J/ψ production: ep → ep J/ψ

$$x_V = (Q2 + M_V^2)/(2P \cdot q)$$

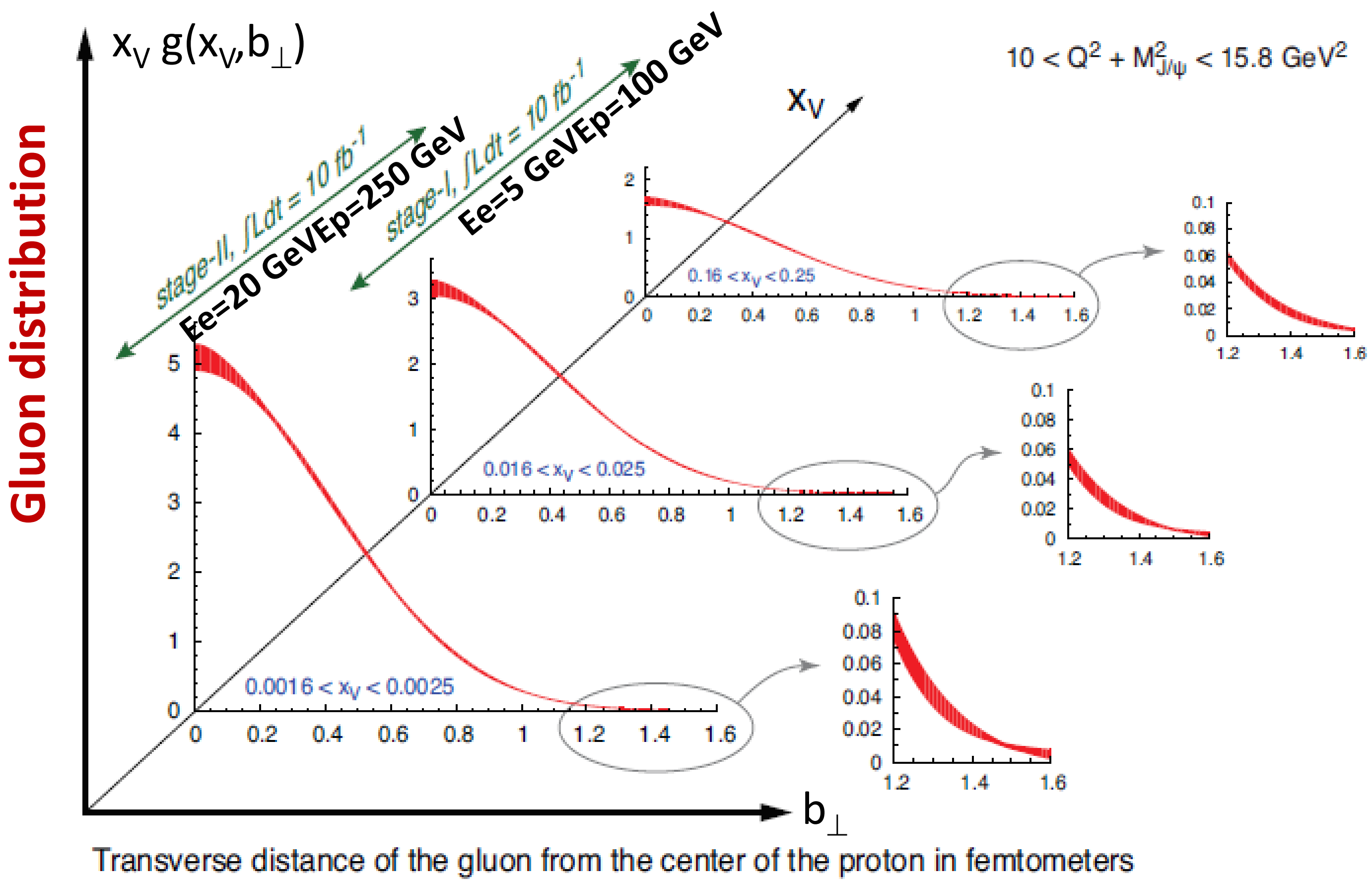

exclusive Υ production at EIC

mapping in the transverse plane
Impact parameter distribution

$$q_f(x, b_\perp) = \int \frac{d^2\Delta_\perp}{(2\pi)^2} e^{-i\Delta_\perp \cdot b_\perp} H_f(x, 0, -\Delta_\perp^2)$$

$$\langle b_\perp^2 \rangle^q(x) = -4 \frac{\partial}{\partial \boldsymbol{\Delta}_\perp^2} \ln H^q(x, 0, -\boldsymbol{\Delta}_\perp{}^2)\Big|_{\boldsymbol{\Delta}_\perp = 0}$$

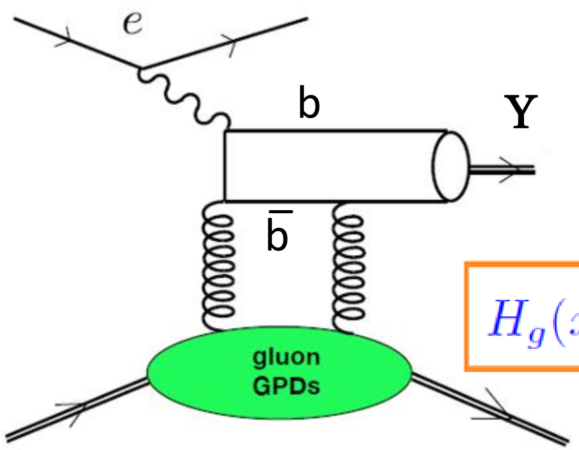

$$H_g(x), E_g(x)$$

Exclusive Υ production: ep → ep Υ

$$x_V = (Q2 + M_V^2)/(2P \cdot q)$$

Gluon distribution with 100 fb^{-1}

$$89.5\ \text{GeV}^2 < Q^2 + M^2 < 91\ \text{GeV}^2$$

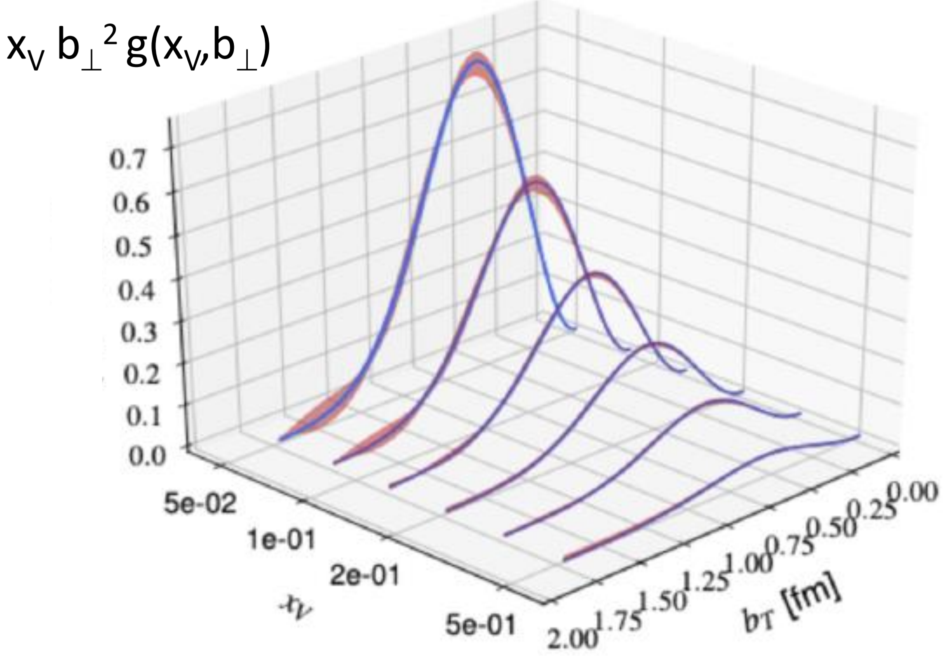

Medium energy is the best

Ee=10 GeVEp=100 GeV with one year of $\int L = 100 fb^{-1}$ $L = 10^{34} cm^{-2} s^{-1}$

Coherent DVCS on ^{4}He

Impact of pT threshold for the recoil detection

pT=0.1 GeV pT=0.2 GeV pT=0.3 GeV

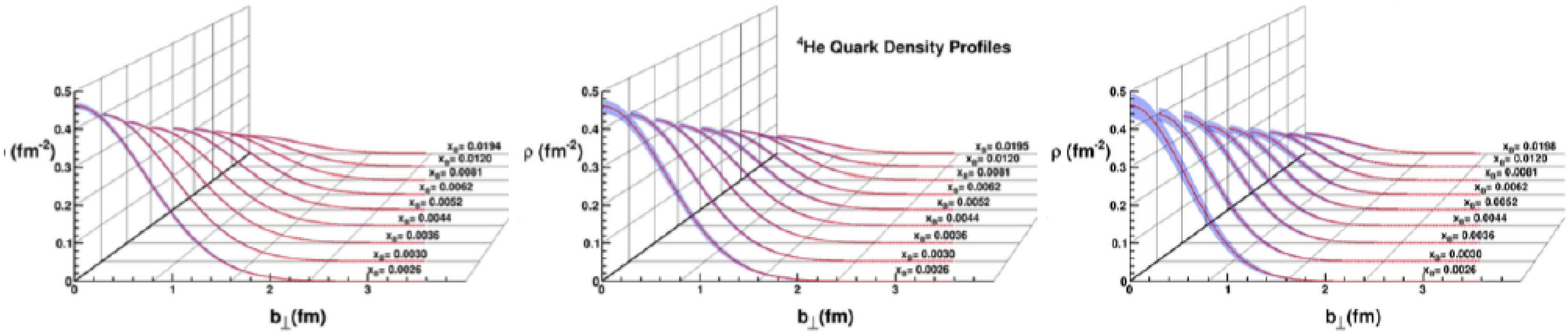

Quark density profiles for coherent DVCS off ^{4}He generated with TOPEG. Extraction based on fit using leading-order formalism and three Roman Pot p_T thresholds: 0.1 (left), 0.2 (centre) and 0.3 GeV (right).

Minimum reach in -t directly affects the uncertainties on the density profiles.

EIC detector requirements

Acceptance close to 4π with $-4 < \eta < 4$

pseudorapidity $\eta \equiv -\ln\left[\tan\left(\frac{\theta}{2}\right)\right]$

Detector 1 called EPIC being finalized

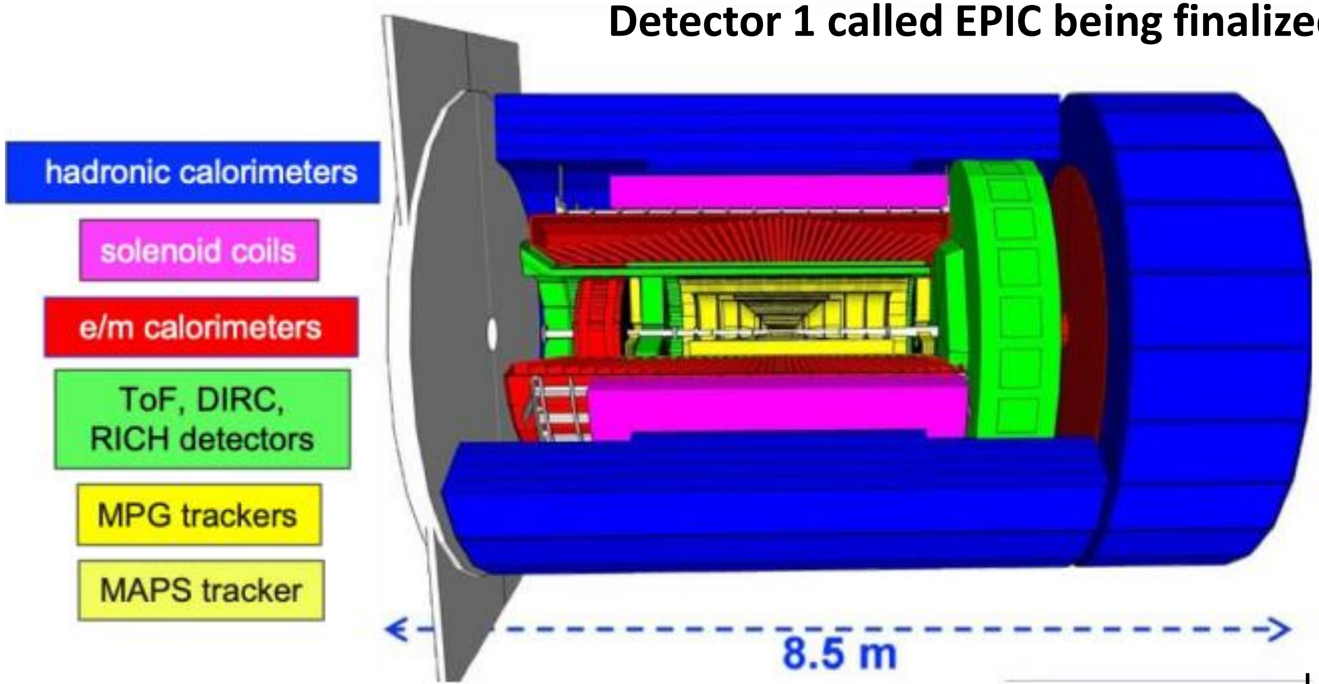

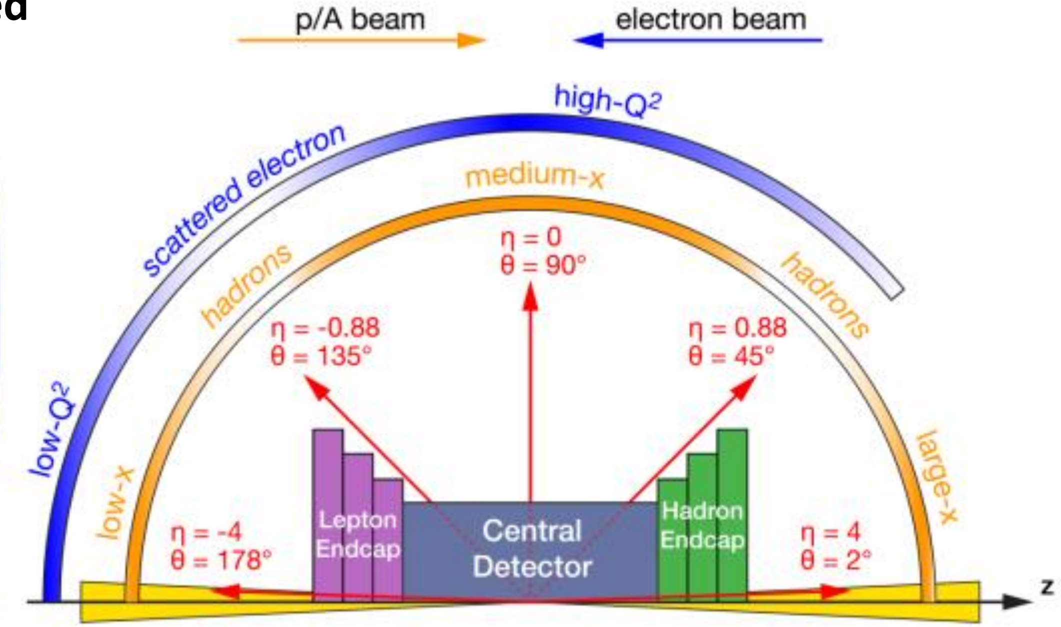

- High precision low mass tracking
  - small (μ-vertex Silicon) MAPS Monolithic Active Pixel Sensors
  - large radius tracking with MPG micro Pattern Gaseous detectors
- Particle Identification
  - ToF Time Of Flight
  - RICH Ring Imaging Cerenkov
  - DIRC Detection of Internally Reflected Cerenkov
- Energy measurement with calorimeters

Low Q2 scattered electrons
Bethe-Heitler photons
For luminosity

Neutrons, scattered protons, ions from diffractive reactions

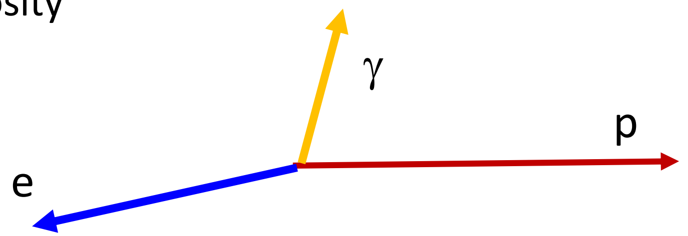

When $Q^2 \searrow$ or $\sqrt{s} \nearrow$ more focused on the beam axis

Forward and backward detectors

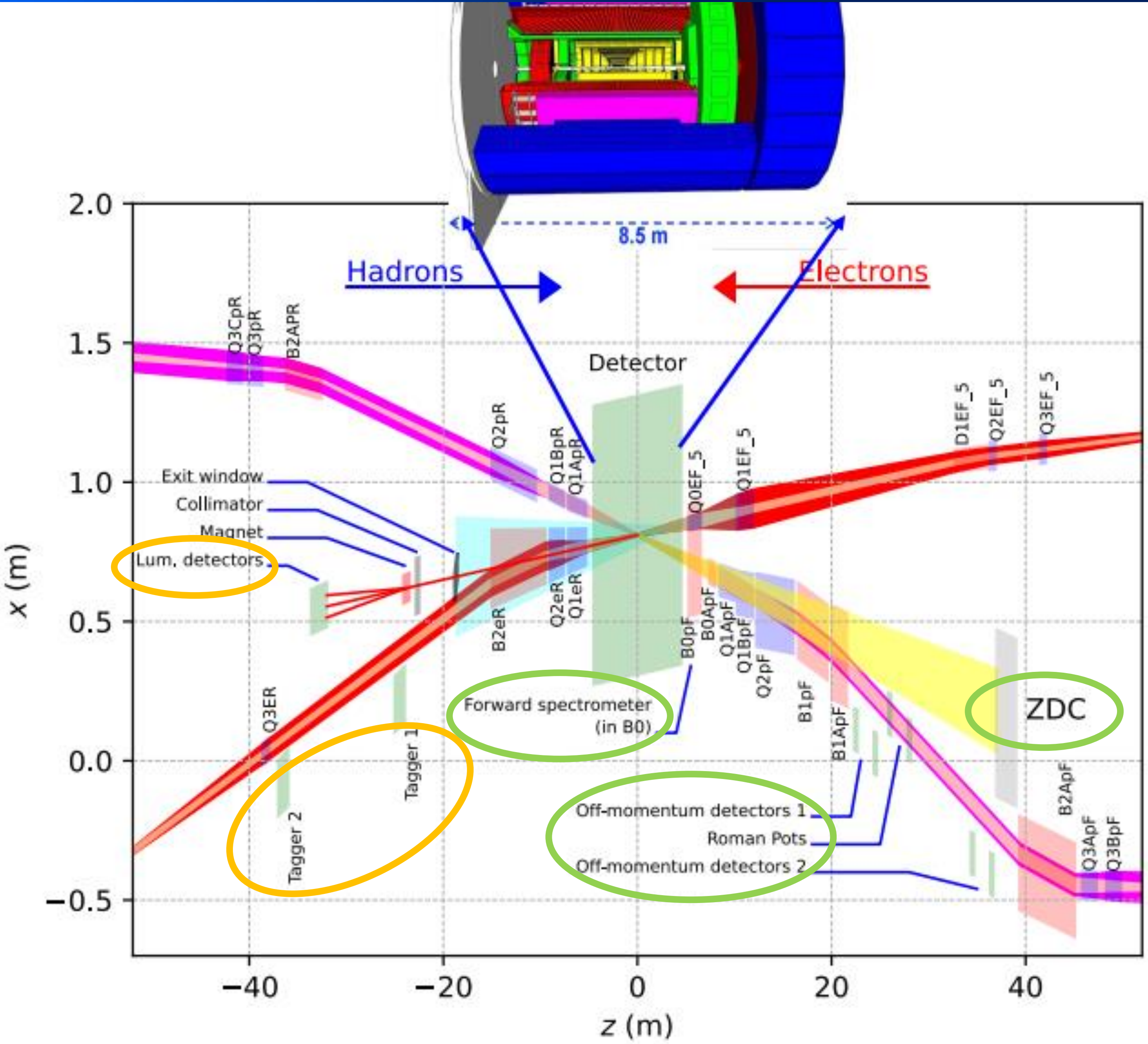

Total size detector: ~75m
Central detector: ~10m
Backward electron detection: ~35m
Forward hadron spectrometer: ~40m

Auxiliary detectors needed to tag particles with very small scattering angles both in the outgoing lepton and hadron beam direction (B0-Taggers, Off-momentum taggers, Roman Pots, Zero-degree Calorimeter and low Q2-tagger).

- For low Q^2 coverage
- To capture forward going protons and neutrons and decay product of Δ, Λ

Forward detectors

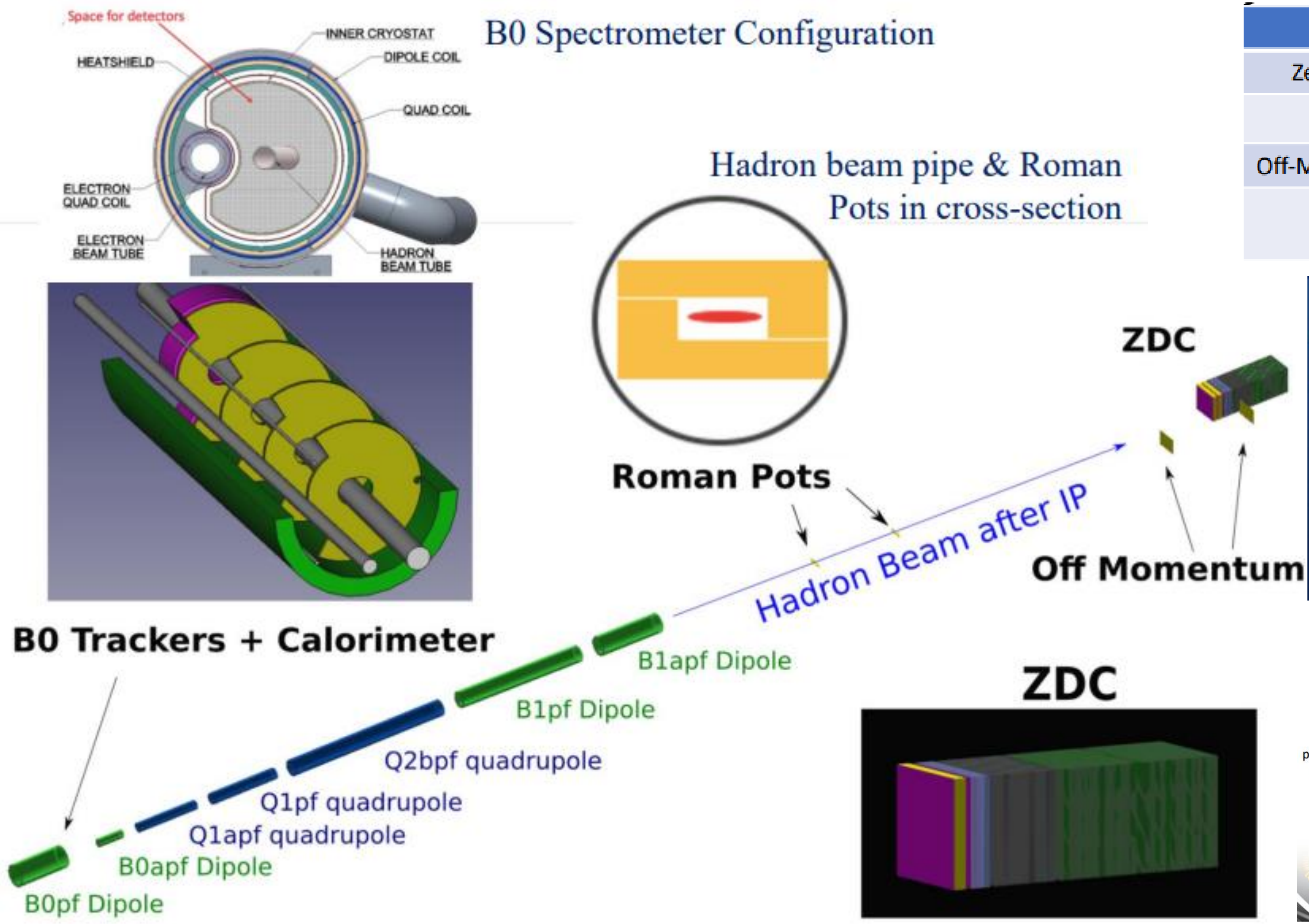

Detector	Acceptance
Zero-Degree Calorimeter (ZDC)	$\theta < 5.5$ mrad ($\eta > 6$)
Roman Pots (2 stations)	0.0* $< \theta < 5.0$ mrad ($\eta > 6$)
Off-Momentum Detectors (2 stations)	$0.0 < \theta < 5.0$ mrad ($\eta > 6$)
B0 Detector	$5.5 < \theta < 20.0$ mrad ($4.6 < \eta < 5.9$)

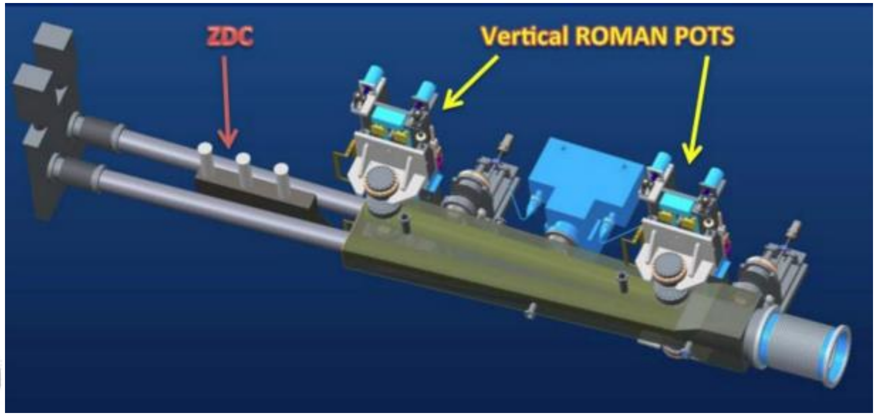

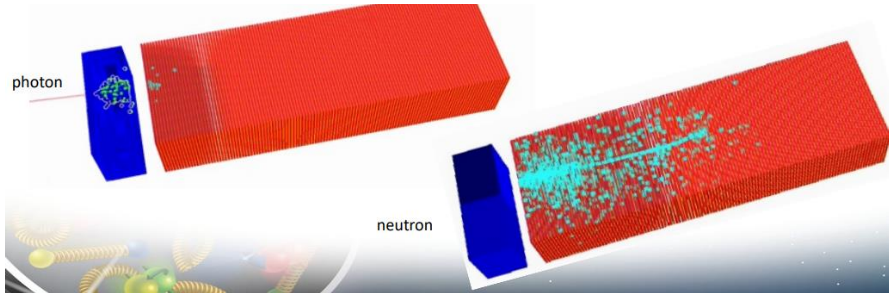

EIC project: Luminosity VS Center of Mass Energy

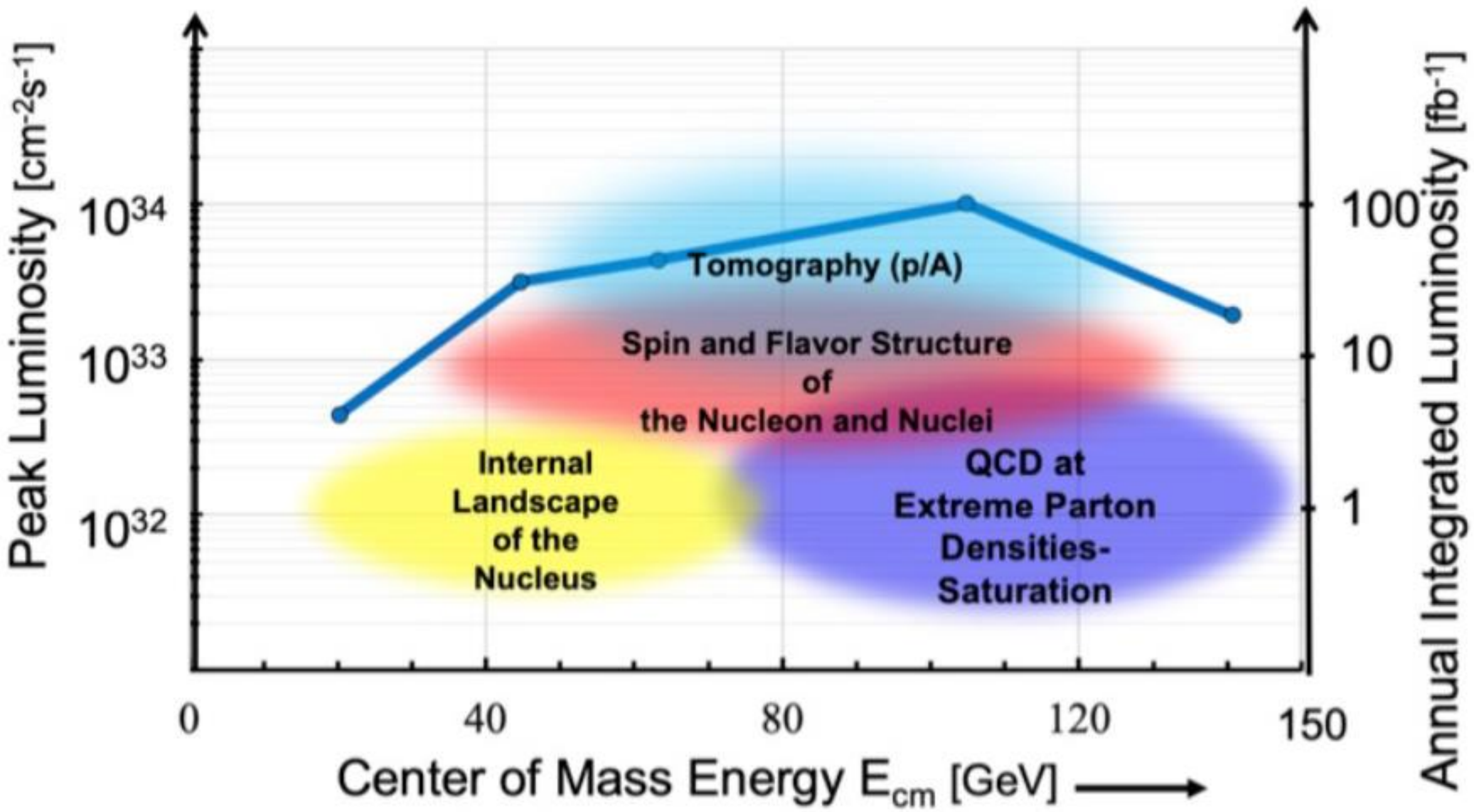

EIC project: Luminosity VS Center of Mass Energy

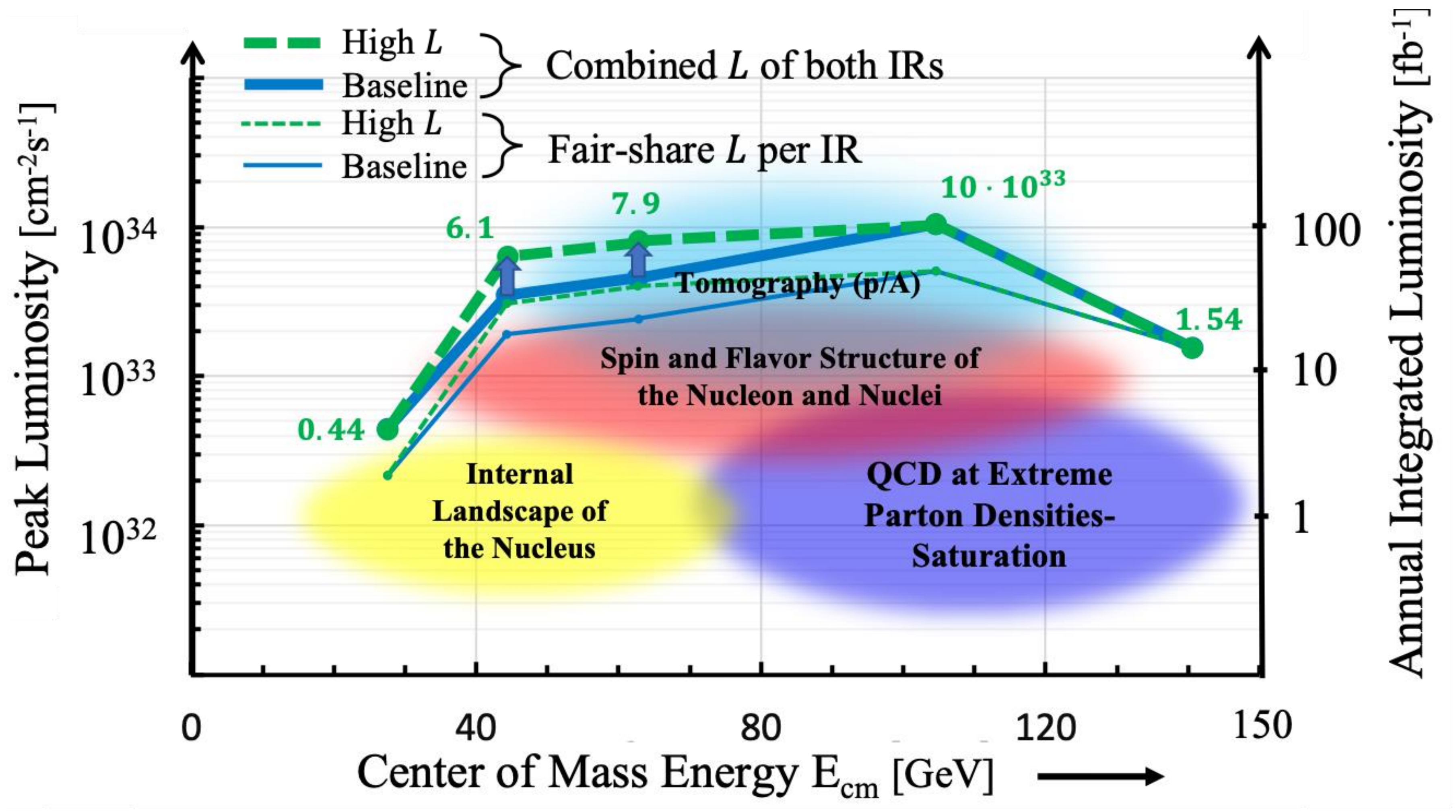

EIC Luminosity VS the other facilities in the world

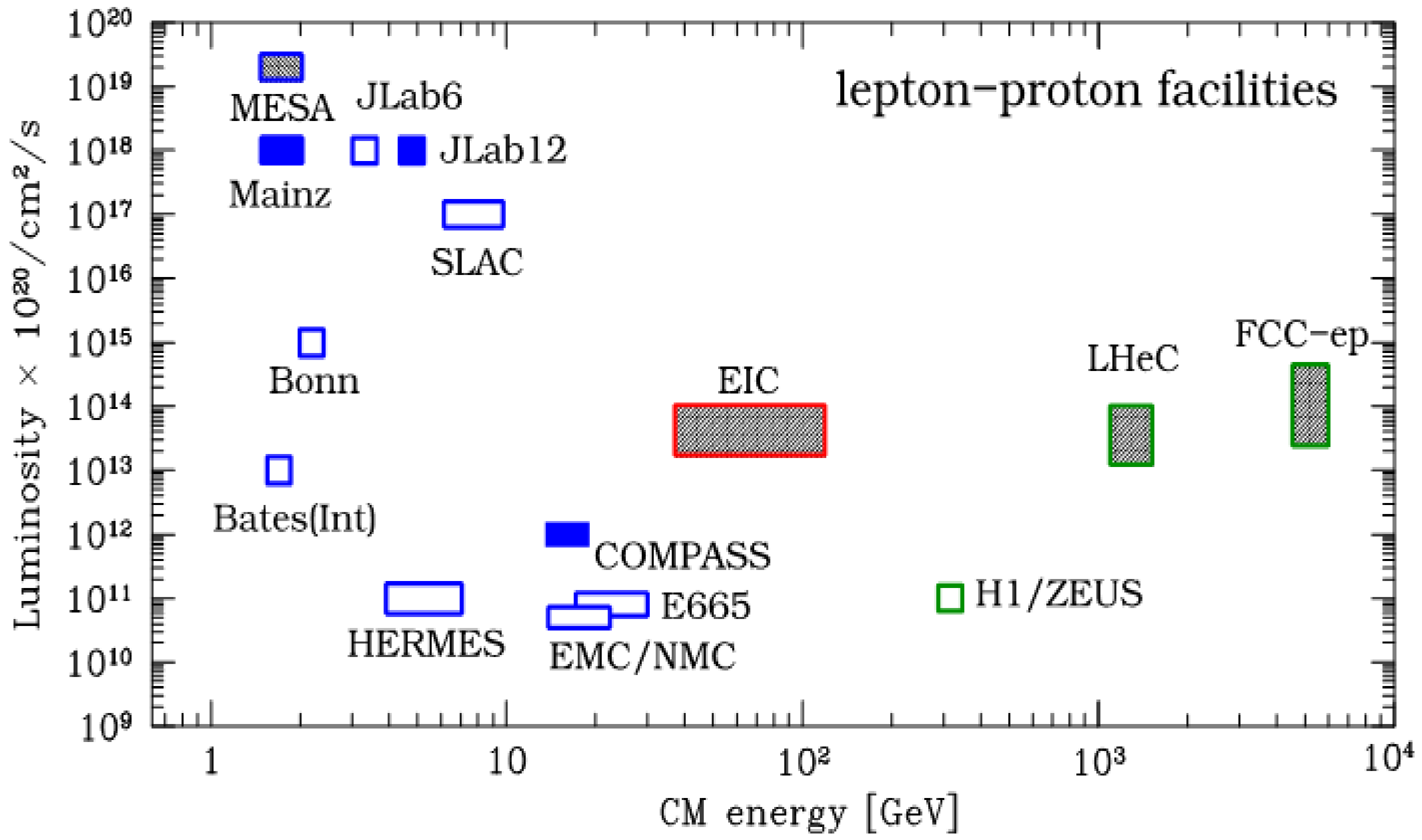

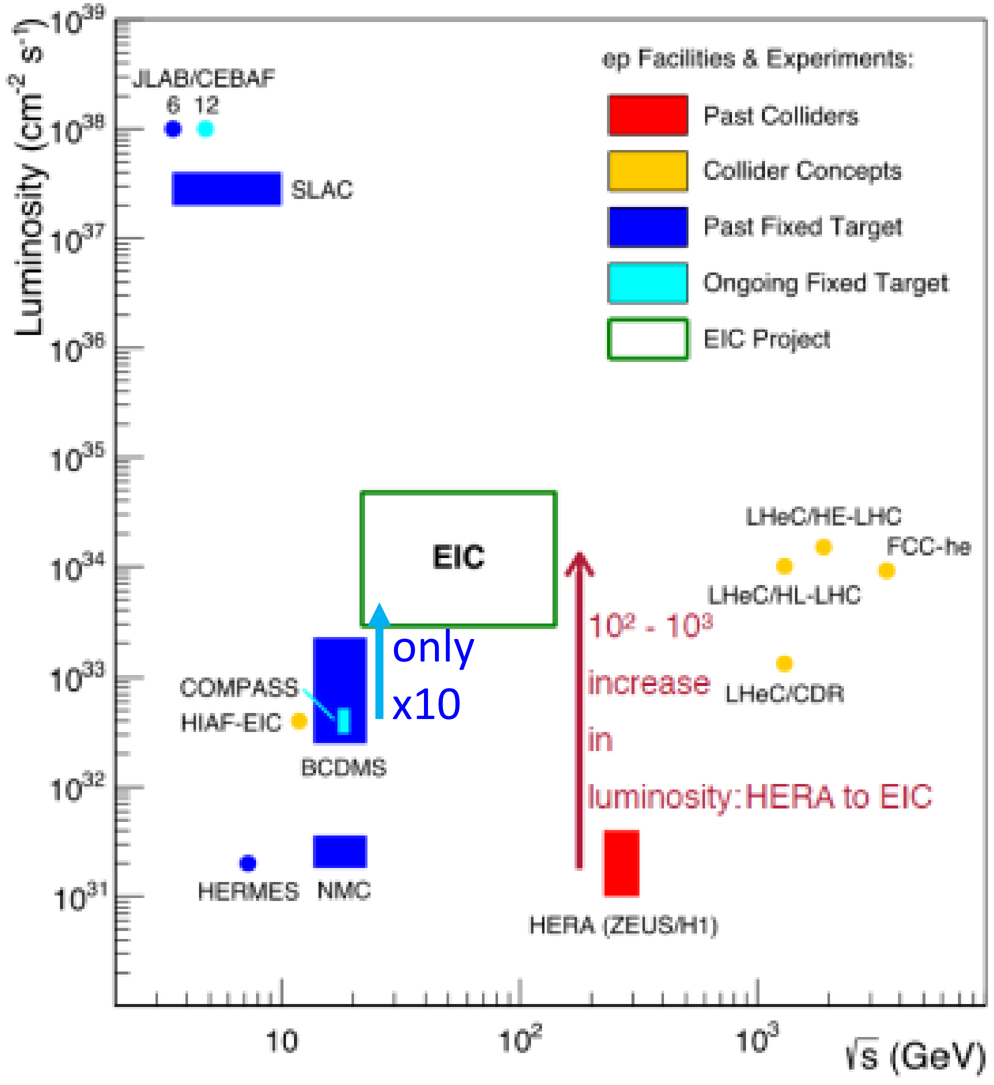

The ideal experiment for exclusive reaction

High beam energy

ensure hard regime and large kinematic domain
polarized beam (polarization >70%)
availability of **positive** and **negative** leptons
variable energy for:
- L/T separation for pseudo scalar production
- ε separation for $DVCS^2$ and Interf DVCS

H_2, D_2 and nuclear target, Long. Pol., Transv. Pol. Target

High luminosity (10^{33} to 10^{34} $cm^{-1}s^{-1}$)

small cross section
fully differential analysis (x_B, Q^2, t, ϕ)
With 10^{33} $cm^{-2}s^{-1}$, the integrated luminosity achieved with 30 weeks operation is 10 fb^{-1}
GPD would ask for 100 fb^{-1} in 1 year ➔ need of the highest luminosity of 10^{34} $cm^{-2}s^{-1}$

Hermetic detectors

ensure exclusivity - careful design of the IP and hadron beam parameters for $0.02 < |t| < 1.6$ GeV^2

Compton Scattering at EIC

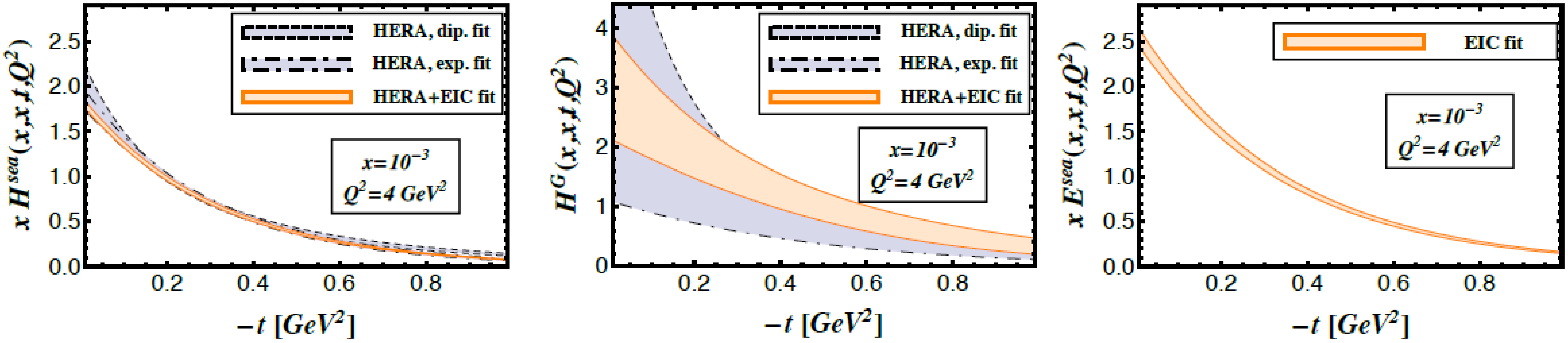

The violet band is the uncertainty obtained excluding the EIC pseudo-data from the global fit procedure.

DVCS, TCS:

- Consistency of factorization
- Test of universality
- Better determination of ReH

Reference Detector – Backward/Forward Detectors

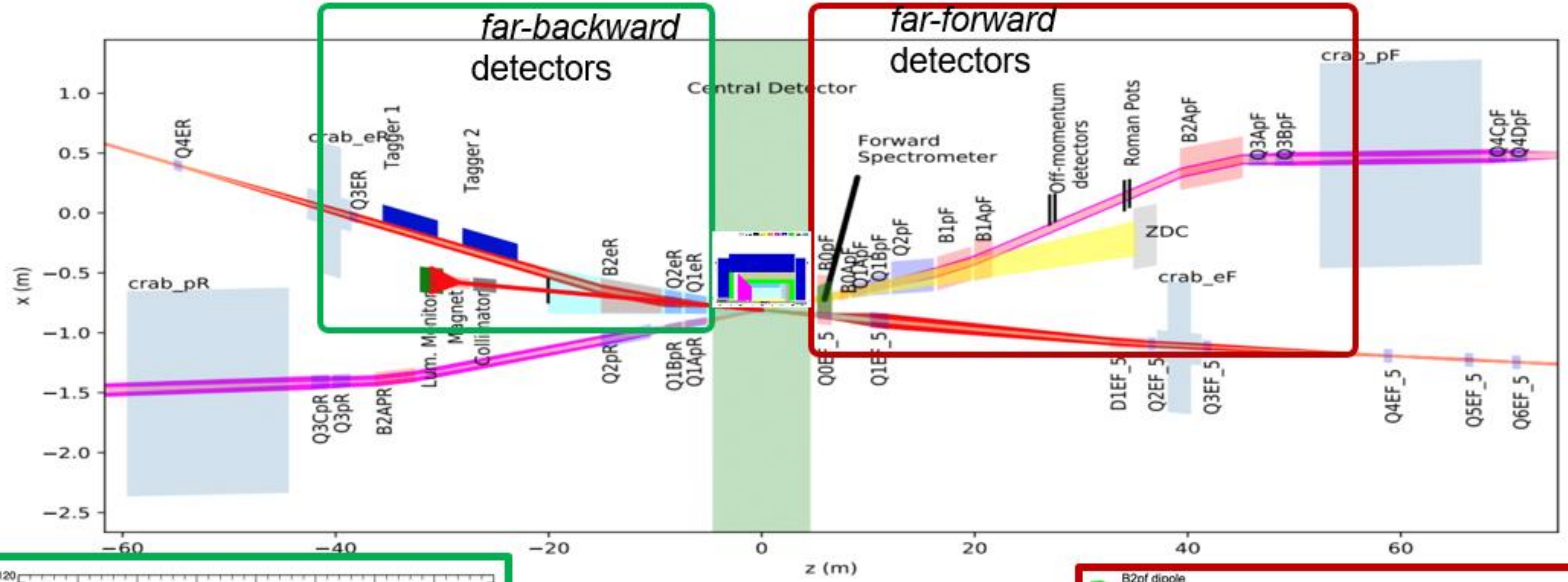

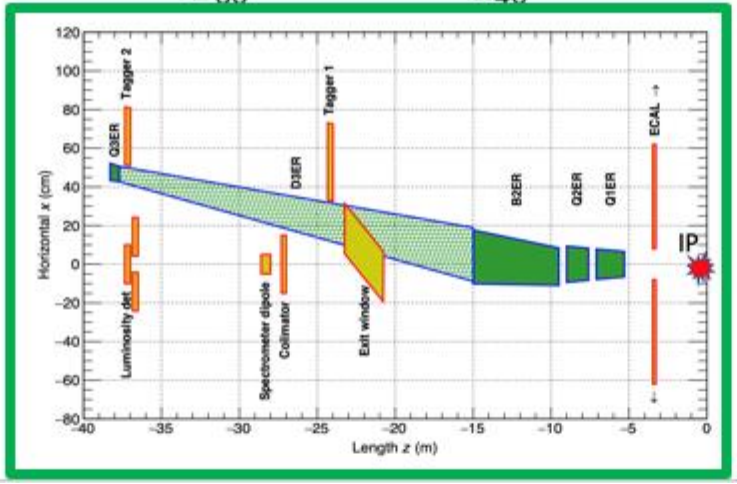

Extensive integration of forward and backward detector elements into the accelerator lattice

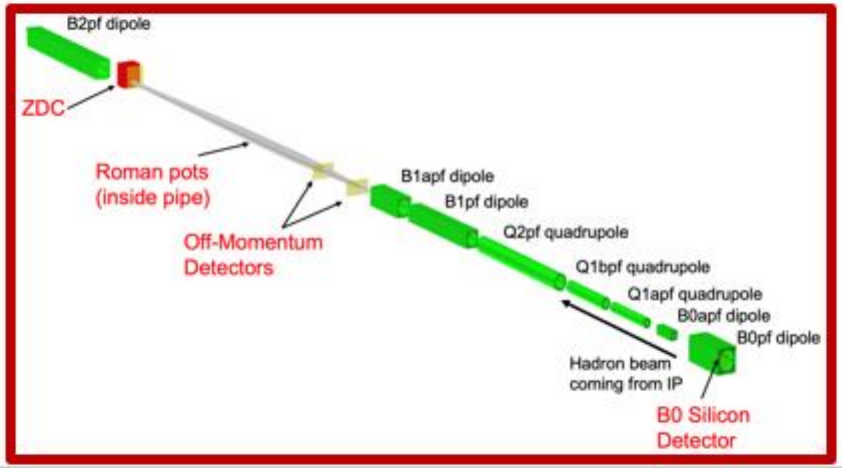

Off-Momentum Detectors

- Off-momentum protons → smaller magnetic rigidity → **greater bending in dipole fields.**
- **Important for any measurement with nuclear breakup!**

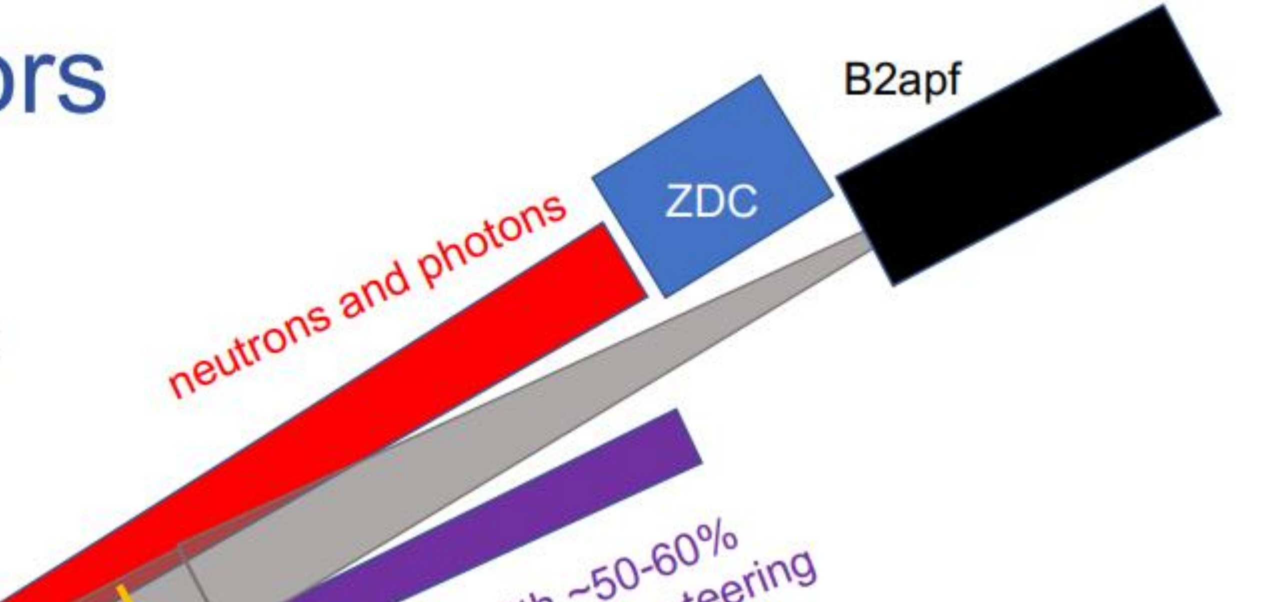
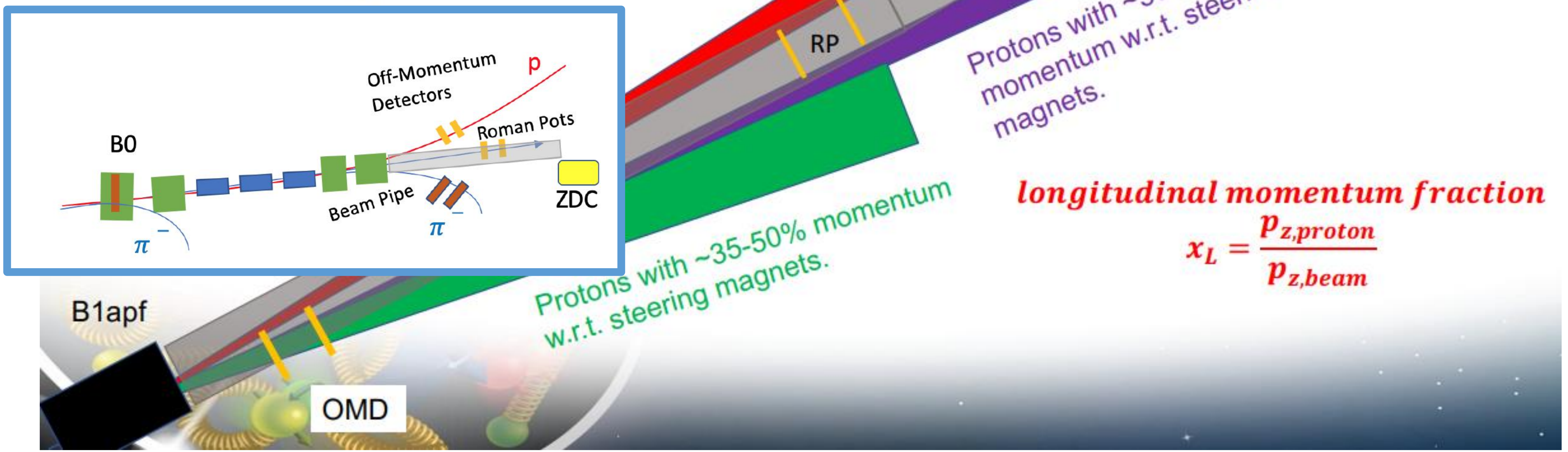

High resolution timing technologies

- *(AC)-LGAD*

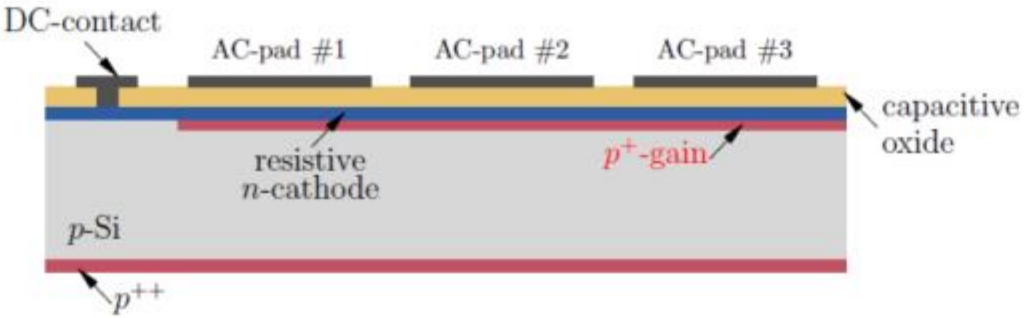

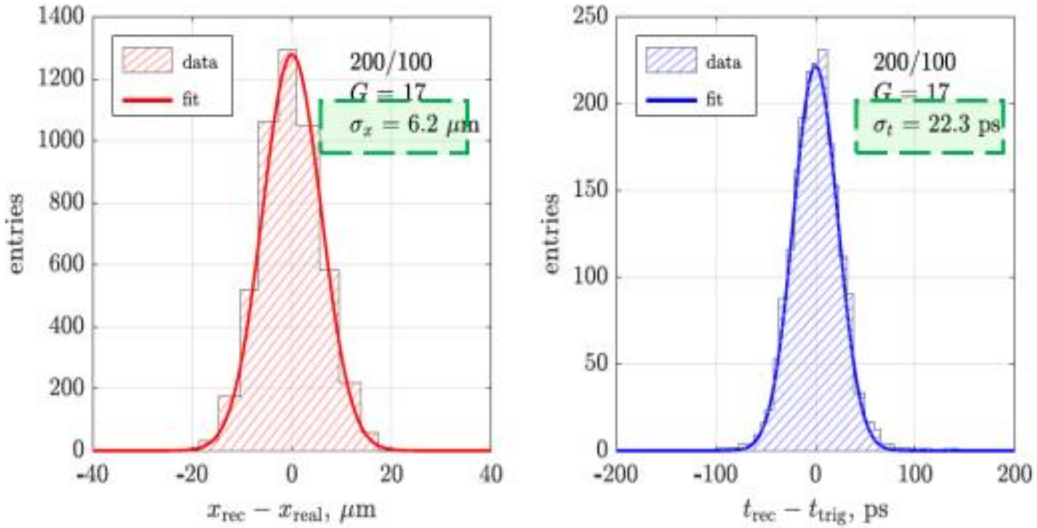

- Detectors can provide <20ps / layer
- moderate granularity (500x500μm^2)
- AC-coupled variety gives 100% fill factor

B0 : Space for detectors

- For far-forward area:
  Roman Pots,
  Off-momentum detectors,
  B0-detectors (in combination with high resolution Si-pixels)

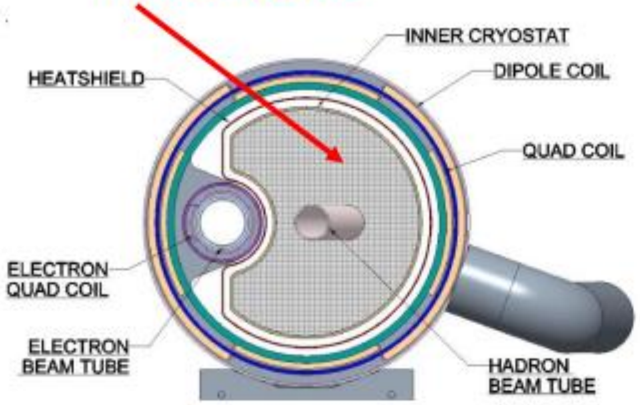

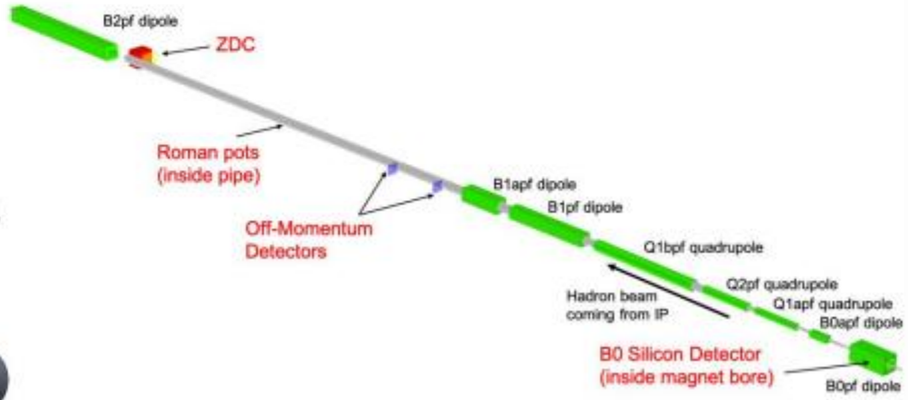

Julia

$$D^{*+} \to D^0 \pi_s^+ \to (K^- \pi^+) \pi_s^+$$

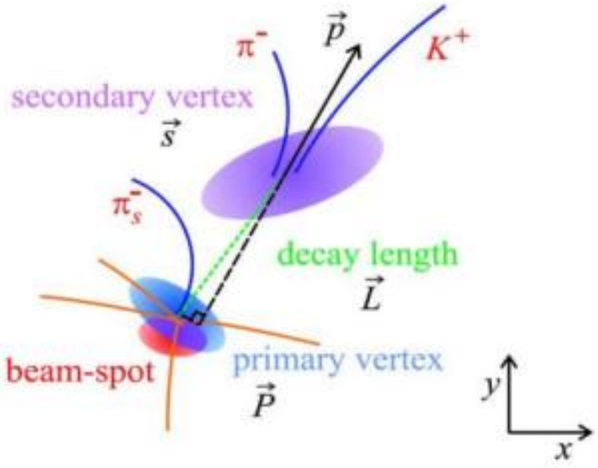

$$R(m) = \frac{P_T(GeV)}{0.3 \cdot B(T)}$$

Diffraction events & gluon densities

Diffraction cross-sections have strong discovery potential:

High sensitivity to gluon density in linear regime: $\sigma \sim [g(x,Q^2)]^2$

Dramatic changes in cross-sections with onset of non-linear strong color fields

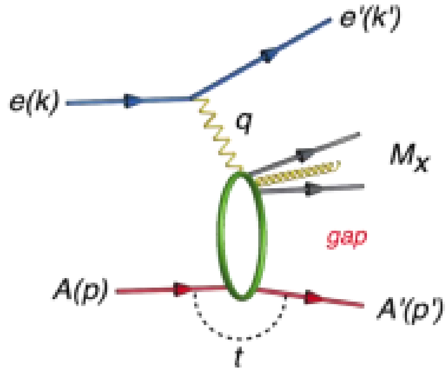

Extracting the gluon distribution $\rho(b_T)$ of nuclei via Fourier transformation of $d\sigma/dt$ in diffractive J/ψ production

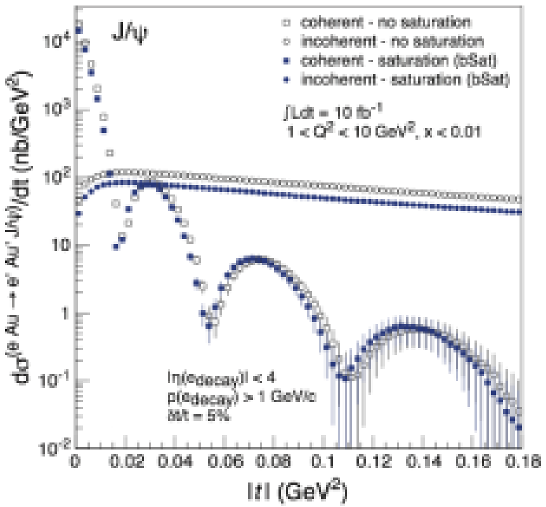

Probing gluon saturation through measuring $\sigma_{diff}/\sigma_{tot}$

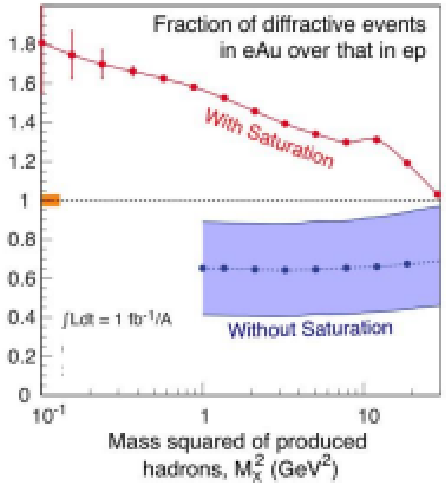

Probing Q^2 dependence of gluon saturation in diffractive vector meson production